

10 CFR 50.90

December 18, 2009

U.S. Nuclear Regulatory Commission  
ATTN: Document Control Desk  
Washington, DC 20555-0001

Peach Bottom Atomic Power Station, Units 2 and 3  
Renewed Facility Operating License Nos. DPR-44 and DPR-56  
NRC Docket Nos. 50-277 and 50-278

Subject: Revised Criticality Analysis - Revision to Technical Specification 4.3.1.1.a  
Concerning k-infinity

- References:
- 1) Letter from P. B. Cowan (Exelon Generation Company, LLC) to U.S. Nuclear Regulatory Commission, "License Amendment Request – Revision to Technical Specification 4.3.1.1.a Concerning k-infinity," dated June 25, 2008
  - 2) Letter from J. D. Hughey (U.S. Nuclear Regulatory Commission) to P. B. Cowan (Exelon Generation Company, LLC), "Peach Bottom Atomic Power Station, Unit Nos. 2 and 3: Request for Withholding Information From Public Disclosure (TAC NOS. MD9154 and MD9155)" (concerning the Northeast Technology Corporation submittal), dated October 10, 2008
  - 3) Letter from J. D. Hughey (U.S. Nuclear Regulatory Commission) to P. B. Cowan (Exelon Generation Company, LLC), "Peach Bottom Atomic Power Station, Unit Nos. 2 and 3: Request for Withholding Information From Public Disclosure (TAC NOS. MD9154 and MD9155)" (concerning the Global Nuclear Fuel submittal), dated October 10, 2008
  - 4) Letter from P. B. Cowan (Exelon Generation Company, LLC) to U.S. Nuclear Regulatory Commission, "Response to Request for Additional Information – Revision to Technical Specification 4.3.1.1.a Concerning k-infinity," dated November 6, 2008

- 5) Letter from J. D. Hughey (U.S. Nuclear Regulatory Commission) to P. B. Cowan (Exelon Generation Company, LLC), "Peach Bottom Atomic Power Station, Unit Nos. 2 and 3: Request for Withholding Information From Public Disclosure (TAC NOS. MD9154 and MD9155)," dated December 29, 2008
- 6) Letter from J. D. Hughey (U.S. Nuclear Regulatory Commission) to P. B. Cowan (Exelon Generation Company, LLC), "Peach Bottom Atomic Power Station, Unit Nos. 2 and 3: Request for Proprietary Review of Request for Additional Information Regarding License Amendment Request to Revise Technical Specification 4.3.1.1.a Concerning k-infinity (TAC NOS. MD9154 and MD9155)," dated January 21, 2009
- 7) Letter from P. B. Cowan (Exelon Generation Company, LLC) to U.S. Nuclear Regulatory Commission, "Response to Request for Additional Information - Revision to Technical Specification 4.3.1.1.a Concerning k-infinity," dated March 9, 2009
- 8) Letter from J. D. Hughey (U.S. Nuclear Regulatory Commission) to P. B. Cowan (Exelon Generation Company, LLC), "Peach Bottom Atomic Power Station, Units 2 and 3: Request for Withholding Information From Public Disclosure (TAC NOS. MD9154 and MD9155)" (concerning NET-264-02, Rev. 1), dated May 13, 2009
- 9) Letter from J. D. Hughey (U.S. Nuclear Regulatory Commission) to P. B. Cowan (Exelon Generation Company, LLC), "Peach Bottom Atomic Power Station, Unit Nos. 2 and 3: Request for Withholding Information From Public Disclosure (TAC NOS. MD9154 and MD9155)" (concerning NET-264-02, Rev. 2, NET-264-03, Rev. 0, and Response to RAI), dated May 13, 2009
- 10) Letter from P. B. Cowan (Exelon Generation Company, LLC) to U.S. Nuclear Regulatory Commission, "Response to Request for Additional Information - Revision to Technical Specification 4.3.1.1.a Concerning k-infinity," dated June 12, 2009
- 11) Letter from J. D. Hughey (U.S. Nuclear Regulatory Commission) to P. B. Cowan (Exelon Generation Company, LLC), "Peach Bottom Atomic Power Station, Unit Nos. 2 and 3: Request for Withholding Information From Public Disclosure (TAC NOS. MD9154 and MD9155)" (concerning NET-264-02 P, Rev. 1), dated September 16, 2009
- 12) Letter from J. D. Hughey (U.S. Nuclear Regulatory Commission) to P. B. Cowan (Exelon Generation Company, LLC), "Peach Bottom Atomic Power Station, Unit Nos. 2 and 3: Request for Withholding Information From Public Disclosure (TAC NOS. MD9154 and MD9155)," (concerning NET-264-02, Rev. 3, NET-264-03, Rev. 1, and Response to RAI, Rev. 1), dated September 16, 2009

In the Reference 1 letter, Exelon Generation Company, LLC (Exelon) requested an amendment to Appendix A, Technical Specifications, of the Renewed Facility Operating Licenses DPR-44 and DPR-56. The proposed change would revise the maximum k-infinity value contained in Technical Specification 4.3.1.1.a for the storage of fuel assemblies in the spent fuel storage racks. Additional correspondence concerning this issue is identified in References 2 through 12.

As a result of a meeting between Exelon and U. S. Nuclear Regulatory Commission Staff on June 16, 2009, a revised criticality analysis utilizing a less reactive fuel bundle is being provided by December 18, 2009, to support the current license amendment. This criticality analysis assumes a peak panel average Boraflex degradation loss, and provides a discussion on ensuring that this loss will not be exceeded through ongoing BADGER and RACKLIFE testing and degradation monitoring. This less reactive bundle results in revised tolerances, uncertainties and biases to ensure k-effective remains below 0.95. Attachment 1 to this letter contains this revised criticality analysis. Attachment 2 contains the non-proprietary version of this analysis.

Attachment 3 evaluates the bundles built for Peach Bottom Atomic Power Station (PBAPS), Units 2 and 3 on a cold, uncontrolled, in-core k-infinite basis, and identifies the limiting lattices. A revised k-infinity value was calculated based on a bounding fuel bundle design utilizing a TGBLA06 methodology. Certain bounding fuel bundle design parameters from this analysis were utilized in the revised criticality analysis. The Attachment 3 analysis provides a revised k-infinity value of 1.270.

The revised criticality analysis contained in Attachment 1 is based upon an assumed peak panel average Boraflex degradation loss. Therefore, the characterization of the Boraflex panel degradation provided in the Reference 10 letter (NET-264-03, Revision 1, "Characterization of Boraflex Panel Degradation in the Peach Bottom Unit 2 Spent Fuel Pool Projected to May 2010") is superseded by the information in Attachment 1, and is no longer necessary.

This analysis has conservatively determined that the k-effective value will remain valid through December 2013, based upon an assumed peak panel average Boraflex degradation loss, utilizing current BADGER and RACKLIFE projections. However, ongoing projections may determine that this date can be extended – through 2015 – with prudent spent fuel management. Exelon anticipates submitting a new license amendment package in the second quarter of 2011 which will provide a final resolution to the Boraflex degradation issue.

As a result of the changes provided in the revised criticality analysis, the no significant hazards consideration has been revised. In particular, the previous value for the proposed maximum k-infinity of 1.318 has been revised to 1.270. Attachment 5 contains the revised no significant hazards consideration. Attachment 6 contains revised Technical Specification pages.

Attachment 1 contains information proprietary to NETCO. NETCO requests that the document contained in Attachment 1 be withheld from public disclosure in accordance with 10 CFR 2.390(a)(4). An affidavit supporting this request is also contained in Attachment 1. Attachment 2 contains a non-proprietary version of the NETCO document.

Revised Criticality Analysis - Revision to  
Technical Specification 4.3.1.1.a Concerning k-infinity  
December 18, 2009  
Page 4

Attachment 3 contains information proprietary to Global Nuclear Fuel. Global Nuclear Fuel requests that the document contained in Attachment 3 be withheld from public disclosure in accordance with 10 CFR 2.390(a)(4). An affidavit supporting this request is also contained in Attachment 3. Attachment 4 contains a non-proprietary version of the Global Nuclear Fuel document.

If any additional information is needed, please contact Tom Loomis at (610) 765-5510.

I declare under penalty of perjury that the foregoing is true and correct. Executed on the 18<sup>th</sup> of December 2009.

Respectfully,

*PBK*  
  
\_\_\_\_\_  
Pamela B. Cowan  
Director, Licensing & Regulatory Affairs  
Exelon Generation Company, LLC

- Attachments:
- 1) Proprietary Version of NET-264-02 P, Revision 4, "Criticality Analysis of the Peach Bottom Spent Fuel Racks for GNF 2 Fuel with Maximum Boraflex Panel Degradation"
  - 2) Non-Proprietary Version of NET-264-02 NP, Revision 4, "Criticality Analysis of the Peach Bottom Spent Fuel Racks for GNF 2 Fuel with Maximum Boraflex Panel Degradation"
  - 3) Proprietary Version of GNF-0000-0110-5796-P, Revision 0, "GNF2 Design Basis Bundle for Spent Fuel Criticality Analysis at Peach Bottom Atomic Power Station Units 2 & 3"
  - 4) Non-Proprietary Version of GNF-0000-0110-5796-NP, Revision 0, "GNF2 Design Basis Bundle for Spent Fuel Criticality Analysis at Peach Bottom Atomic Power Station Units 2 & 3"
  - 5) Revised No Significant Hazards Consideration
  - 6) Markup of Proposed Technical Specification Page Changes

cc USNRC Region I, Regional Administrator  
USNRC Senior Resident Inspector, PBAPS  
USNRC Project Manager, PBAPS  
R. R. Janati, Commonwealth of Pennsylvania  
S. T. Gray, State of Maryland

**Attachment 2**

**Non-Proprietary Version of NET-264-02 NP, Revision 4,  
“Criticality Analysis of the Peach Bottom Spent Fuel Racks for  
GNF 2 Fuel with Maximum Boraflex Panel Degradation”**

# Criticality Analysis of the Peach Bottom Spent Fuel Racks for GNF2 Fuel with Maximum Boraflex Panel Degradation

4

Prepared

for

Exelon Nuclear  
Under Purchase Order: 01003029

by:

NETCO, a division of Scientech, a business unit  
of Curtiss-Wright Flow Control Service Corporation  
108 North Front Street  
UPO Box 4178  
Kingston, New York 12402

4

Revision:	Date:	Prepared by:	Reviewed By:	Approved By: (QA)
4	12/17/09	Matt C. Harris	[Signature]	J. P. Mariani

Note: New revision signature sheet initiated due to the fact that Revision 4 of NET-264-02 included a change of title.

This document contains proprietary information of the Exelon Generation Company, LLC, Global Nuclear Fuel-Americas, LLC and NETCO, a division of Scientech, a business unit of Curtiss-Wright Flow Control Service Corporation. It is submitted in confidence and is to be used solely for the purpose of which it is furnished and returned upon request. This document and such information is not to be reproduced, transmitted, disclosed or used otherwise in whole or in part without the prior written authorization of Exelon Generation Company, LLC, Global Nuclear Fuel-Americas, LLC and NETCO, a division of Scientech, a business unit of Curtiss-Wright Flow Control Service Corporation.

4

4

Exelon Generation Company, LLC  
200 Exelon Way  
Kennett Square, PA 19348

Global Nuclear Fuel-Americas, LLC  
3901 Castle Hayne Road  
Wilmington, NC 28401

NETCO, a division of Scientech, a  
business unit of Curtiss-Wright  
Flow Control Service Corporation  
108 North Front Street  
UPO Box 4178  
Kingston, NY 12402

4

## Preface

Exelon Nuclear has requested an updated criticality analysis for the spent fuel racks at Peach Bottom Units 2 and 3. The existing rack design incorporates the neutron absorber material Boraflex for reactivity control, which has been observed to be subject to in-service degradation from the combined effects of gamma radiation and long term exposure to the aqueous pool environment. This updated analysis encompasses all current and historical spent fuel designs, and conservatively establishes that the spent fuel racks remain serviceable through 2013.

In 2000, AEA Technology provided Exelon Nuclear analyses which demonstrated that the regulatory sub-criticality design criterion of  $k_{eff} < 0.95$  would be met, with uniform Boraflex degradation up to 10%, when averaged across all panels in the spent fuel racks (pool panel average). Based upon subsequent BADGER testing and RACKLIFE projections, the Unit 2 spent fuel pool uniform Boraflex degradation exceeded a 10% pool panel average in October 2008. As of October 2009, uniform Boraflex degradation in the Unit 2 spent fuel pool had increased marginally to 11.1% pool panel average, with a maximum single panel degradation (peak panel) of 30.3% (as calculated by RACKLIFE). Equivalent values for the Unit 3 spent fuel pool as of October 2009 are 9.7% and 20.6%, respectively. However, a large reactivity margin still remains between Technical Specification 4.3.1.1.a (maximum  $k_{\infty} = 1.362$  cold, uncontrolled, in-core configuration) and fuel used at Peach Bottom (maximum  $k_{\infty}$  at peak reactivity conditions for any fuel assembly operating or in storage at Peach Bottom Units 2 and 3, less than 1.235), providing significant margin to the regulatory sub-criticality design criterion with the additional Boraflex degradation.

By reducing the peak reactivity of the bundle design used in the criticality analysis to  $k_{\infty} = 1.270$  – maintaining a 3.5% reactivity margin for future core designs – it is demonstrated that additional uniform Boraflex degradation may be tolerated (up to [ ]% pool panel average, corresponding to [ ]% peak panel), while maintaining the  $k_{eff} < 0.95$  regulatory criterion and serviceability of the spent fuel racks.

This report addresses the two fundamental areas required to support a change to Technical Specification 4.3.1.1.a. Sections 3 and 4 analyze uniform Boraflex degradation to determine the change in calculated pool reactivity as a function of Boraflex loss. Five data points as a function of reactivity have been determined in order to allow interpolation between 0% and 100% uniform Boraflex degradation. At the end of 2013, RACKLIFE calculations show a [ ]% pool panel average, with a corresponding [ ]% peak panel uniform Boraflex loss, for Peach Bottom Unit 2 (which bounds the Boraflex degradation for Unit 3).

Sections 5 and 6 describe the criticality analysis, which conservatively assumed all panels have a uniform Boraflex loss of [ ]%, and all racks are occupied with fuel bundles at  $k_{\infty} = 1.270$  cold, uncontrolled, in-core configuration. The spent fuel pool rack  $k_{eff}$  calculated in this manner results in a conservative estimate of rack reactivity.

**Table of Contents**

1.0	Introduction.....	1
2.0	Peach Bottom Spent Fuel Racks.....	3
2.1	Spent Fuel Rack Description .....	3
3.0	RACKLIFE Projections .....	6
3.1	Model Overview and Assumptions.....	6
3.2	Future Projections.....	7
4.0	The Reactivity Effects of Boraflex Degradation .....	15
4.1	Introduction .....	15
4.1.1	Uniform Dissolution .....	15
4.1.2	Shrinkage, Including Gaps .....	15
4.1.3	Local Dissolution .....	16
4.2	Methodology for Projecting Future Panel Conditions.....	16
4.3	Methodology for Assessing the Reactivity Effects of Boraflex Degradation .....	20
4.4	Results.....	22
5.0	Results of the Criticality Analysis.....	27
5.1	Design Basis and Design Criteria .....	27
5.2	Analytical Methods and Assumptions .....	28
5.3	Calculated Results.....	32
5.3.1	Reference Eigenvalue Calculations .....	32
5.3.2	CASMO-4 and KENO V.a Reactivity Calculations in-Core and in- Rack Geometries .....	36
5.3.3	Effect of Tolerances and Uncertainties .....	38
5.3.4	Space Between Modules .....	41
5.3.5	Summary of Reactivity Calculations.....	41
5.3.6	Abnormal/Accident Conditions .....	41
6.0	Conclusions .....	44
7.0	References .....	45

Appendix A: NET-901-02-05, Rev 4, Benchmarking of Computer Codes for Calculating the Reactivity State of Spent Fuel Storage Racks, Storage Casks and Transportation Casks.

Appendix B: Evaluation of Most Reactive Lattices in the Peach Bottom Spent Fuel Pool

Appendix C: Area of Applicability

**List of Figures**

Figure 2-1:	Peach Bottom 2 Spent Fuel Pool .....	4
Figure 2-2:	Peach Bottom Storage Cell Elements .....	5
Figure 3-1:	Occupied Cells in the Peach Bottom 2 Spent Fuel Storage Racks on February 26, 2006. ....	9
Figure 3-2:	Projected Occupied Cells in the Peach Bottom 2 Spent Fuel Storage Racks through 2013.....	10
Figure 3-3:	Predicted Boron Carbide Loss through February 26, 2006 in the Peach Bottom Spent Fuel Storage Racks.....	11
Figure 3-4:	Panel Absorbed Dose through February 26, 2006 in the Peach Bottom Spent Fuel Storage Racks .....	12
Figure 3-5:	Predicted Boron Carbide Loss through 2013 in the Peach Bottom Spent Fuel Storage Racks .....	13
Figure 3-6:	Panel Absorbed Dose through 2013 in the Peach Bottom Spent Fuel Storage Racks .....	14
Figure 4-1:	Typical Model of a Peach Bottom Boraflex Panel .....	25
Figure 4-2:	Sample Distribution of Panel Degradation Reactivity Effects .....	26
Figure 5-1:	Bias-Corrected, In-Rack Reactivity versus Burnup for the GNF2 Vanished1 Fuel Type in the Peach Bottom Spent Fuel Storage Racks. ...	35

List of Tables

Table 4-1:	Conservative Reactivity Effects of Cracks Undetected by BADGER .....	23
Table 4-2:	Reactivity Effects of Uniform Boraflex Panel Thinning .....	24
Table 4-3:	Reactivity Effects of Degraded Panels.....	24
Table 5-1:	GNF2 Fuel Assembly Description Peach Bottom Nuclear Generating Station.....	34
Table 5-2:	CASMO-4/KENO V.a Reactivity Comparison in Core Geometry: GNF2 Vanished1 Lattice @ [ ] w/o U-235 ([ ]% T.D.), Zero Burnup, 20°C.....	36
Table 5-3:	CASMO-4/KENO V.a Reactivity Comparison in Rack Geometry: GNF2 Vanished1 Lattice @ [ ] w/o U-235 ([ ]% T.D.), Zero Burnup, 20°C.....	36
Table 5-4:	Summary of Criticality Calculation Results (GNF2 Vanished1 Lattice at 20°C).....	43
Table B-1:	Peak Reactivity GNF Lattices in the Peach Bottom Spent Fuel Racks	
Table C-1:	Peach Bottom Area of Applicability	

## 1.0 Introduction

The Peach Bottom spent fuel pool was refitted with high density spent fuel storage racks in 1986. These racks were fabricated by the Westinghouse Corporation and utilize the neutron absorber material Boraflex for reactivity control. Boraflex has been observed to be subject to in-service degradation from the combined effects of gamma radiation from spent fuel and long term exposure to the aqueous pool environment.<sup>[1,2]</sup>

4

To assure acceptable in service Boraflex performance Exelon Nuclear has initiated a multi-faceted surveillance program. This program includes monitoring pool reactive silica levels, BADGER testing<sup>[3]</sup> and tracking the current and projected performance of every panel of Boraflex in the Peach Bottom pools with RACKLIFE<sup>[4,5]</sup>. To date three BADGER test campaigns have been completed in the Unit 2 SFP and two campaigns have been completed in the Unit 3 SFP. A third BADGER test was completed in December 2009 in the Unit 3 pool and a fourth test is scheduled for January 2010 in the Unit 2 pool. The Peach Bottom Unit 2 RACKLIFE model has been validated by the three BADGER campaigns that also show the Unit 2 spent fuel racks bound the Unit 3 spent fuel racks with respect to Boraflex degradation. This model has been used to predict the in-service degradation of each Boraflex panel.

4

4

4

This report documents the application of an advanced methodology developed by Northeast Technology Corp. for assessing the safe storage of a GNF2 Design Basis Fuel (DBF) bundle in the Westinghouse spent fuel racks with degraded Boraflex. This assessment utilizes the results of the most recent Unit 2 BADGER test data sets to establish distributions of local and global panel degradation at the time of the testing. The RACKLIFE results are then used to track the progression of average panel degradation and project the condition of the Boraflex at a future date when the peak panel boron carbide loss reaches [ ] percent. A special algorithm, developed by NETCO, is then applied to the BADGER data to project the local and global panel degradation based on the RACKLIFE prediction of panel average boron carbide loss.

4

4

4

The reactivity effects of future local and global Boraflex degradation have been converted to an equivalent panel thinning using the KENO V.a code. The equivalent panel thinning values so determined are then used in CASMO-4 and KENO V.a models of the peak reactivity lattice of the GNF2 DBF in the Peach Bottom spent fuel racks. The GNF2 fuel type was used as it is more reactive than 7 x 7, 8 x 8, 9 x 9 and other 10 x 10 fuel designs of equivalent loadings used at Peach Bottom and is therefore bounding. This is due to the smaller rod diameter in the GNF2 bundle allowing for more rapid depletion of the gadolinia. Appendix B contains a summary of the associated lattice reactivities for the bounding lattice of each fuel type. In this manner, it has been demonstrated that the limiting GNF2 (Vanished 1) fuel type (at [ ] percent theoretical density) with a maximum average planar enrichment of up to [ ] w/o U-235 and containing [ ] vanished rod locations and a minimum of [ ] gadolinia rods each with a minimum Gd<sub>2</sub>O<sub>3</sub> loading of [ ] w/o and [ ] gadolinia rod at [ ] w/o can be safely stored ( $k_{eff} \leq 0.95$ ) in the Peach Bottom Boraflex racks with [ ] percent peak Boraflex panel degradation. In addition, any future bundle that produces  $k_{inf}$  of 1.270 or less in the standard cold core geometry may also be stored in the racks. The peak panel loss of [ ] percent corresponds to an average panel boron carbide loss of [ ] percent.

4

4

RACKLIFE predictions and BADGER testing will continue to be applied to monitor the actual boron carbide loss in the Peach Bottom spent fuel racks.

**2.0 Peach Bottom Spent Fuel Racks** | 4

2.1 Spent Fuel Rack Description

The spent fuel racks at Peach Bottom are shown in Figure 2-1. The spent fuel pools for both units are mirror images and each pool contains 15 rack modules of varying size for a total capacity of 3819 storage cells. These racks utilize Boraflex as a neutron poison and contain the panels that were selected for BADGER testing<sup>[8]</sup>. | 4

The individual storage cells are formed by creating a checkerboard configuration of square tubes as shown in Figure 2-2. The basic structure of this storage array is a square stainless steel tube [ ] inches thick with a [ ] inch inside dimension and 169 inches in length. Each structural tube has one sheet of Boraflex [ ] inches long, [ ] inches wide, and [ ] inches thick (nominal) positioned on each of the four outside faces. During manufacture, the Boraflex sheets were first attached to [ ] inches thick stainless steel wrapper plates using a Dow silicone sealant that served as an adhesive. The wrapper plates were then tack welded to the structural cell wall. Tack welds are located on approximately [ ]-inch centers along the length of the wrapper plate. As a result of the structural design of the racks, one sheet of Boraflex is positioned between the opposing faces of the fuel assemblies stored in the modules. | 4

To complete the rack module assembly, the structural tubes with Boraflex and stainless steel wrapper plates are welded together at the corners and to a bottom base plate. In this manner, every other storage location is formed by the structural tube and the resultant locations are formed by the four adjacent faces of neighboring structural tubes. The base plates of each module are fitted with leveling feet that rest on the pool floor. | 4

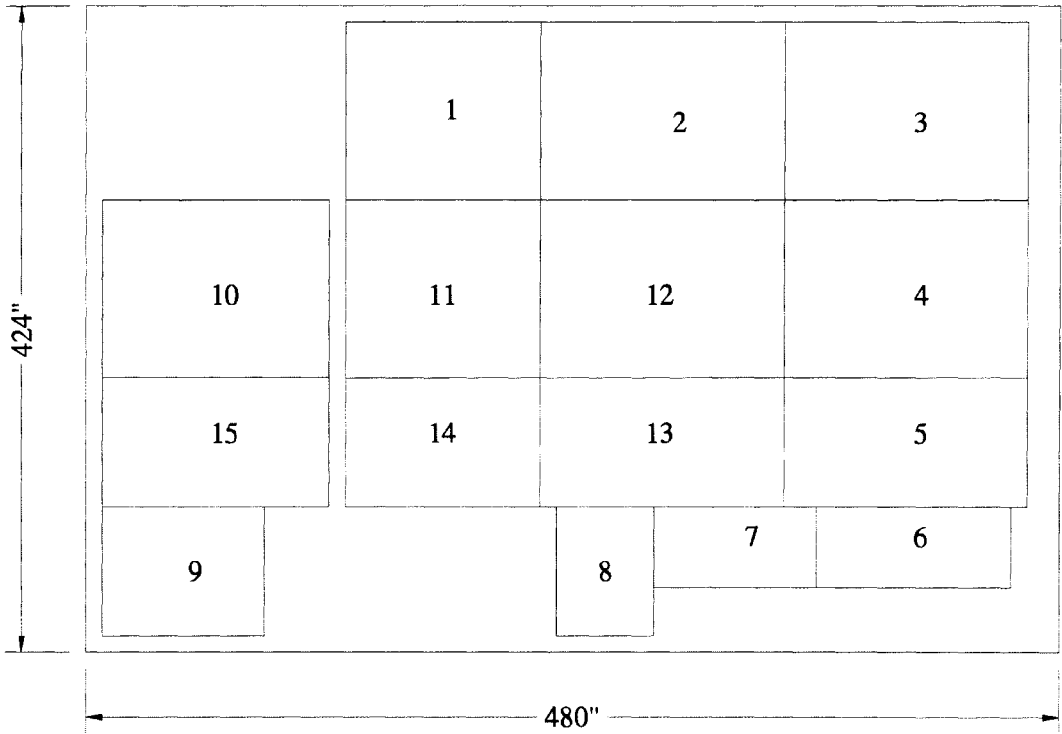


Figure 2-1: Peach Bottom 2 Spent Fuel Pool  
(Note: Numerals are RACKLIFE module designations. Unit 3 is similar.)

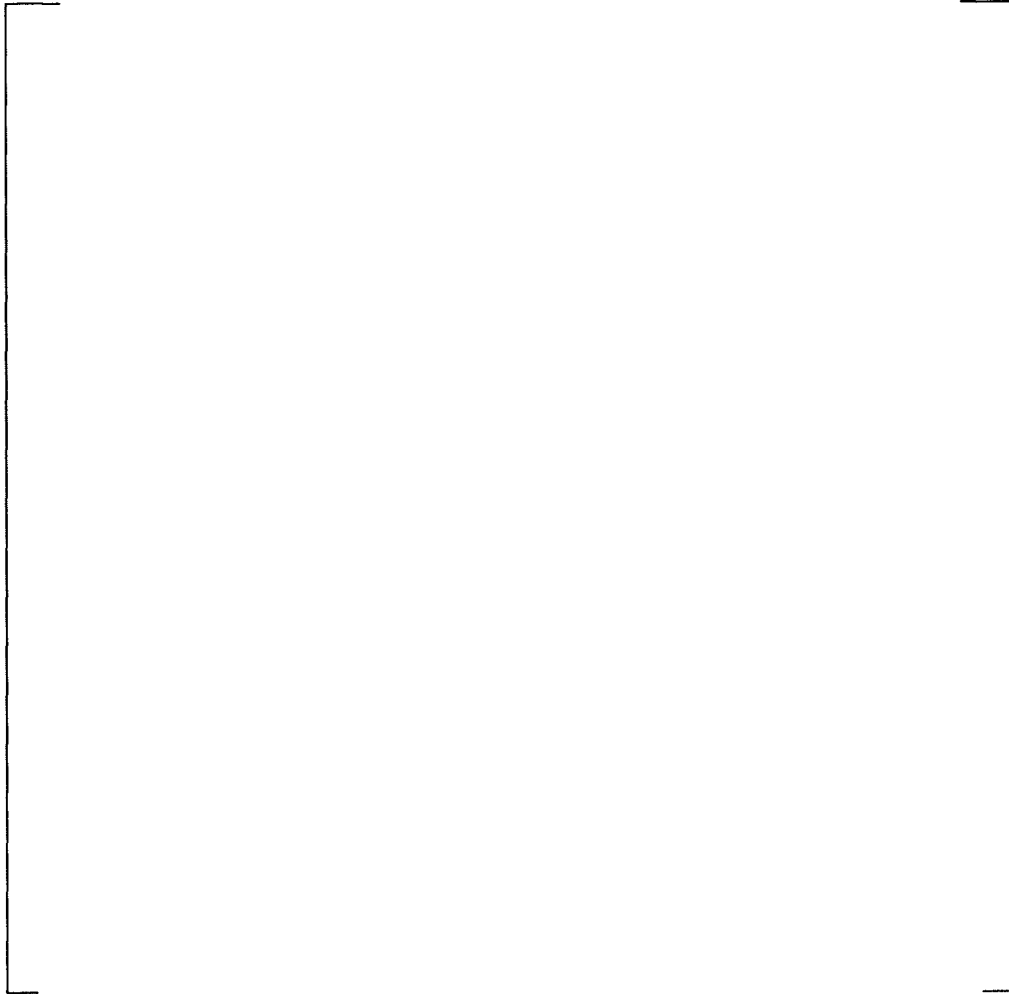


Figure 2-2: Peach Bottom Storage Cell Elements

### 3.0 RACKLIFE Projections

#### 3.1 Model Overview and Assumptions

A RACKLIFE model of the Peach Bottom Unit 2 SFP was originally developed by NETCO and Exelon. The original model was updated by Exelon every 6 months to reflect actual fuel discharges into the spent fuel racks through 2008. The projected outage dates and anticipated fuel discharges (outage and dry cask storage) were updated to project the condition of the Boraflex panels into the future.

4

This model was used to estimate the actual service history of each panel of Boraflex in the Peach Bottom storage racks, including integrated gamma exposure and its condition with respect to B<sub>4</sub>C loss. Information regarding the predicted state of the pool and the condition of the Boraflex at a given time can be determined using the model.

4

#### Reactor Cycle Data

Cycle 17 ended in October 2008. All refueling outage shutdowns were conservatively modeled as an instantaneous shutdown from 100 percent of rated power. Peach Bottom operates on a 2-year fuel cycle, and for modeling purposes it was assumed that the future refueling outages would occur in October 2010 and October 2012. Future reactor shutdowns were also modeled as instantaneous shutdown from 100 percent of rated power. This approach provides a conservative estimate of the gamma exposure to Boraflex panels. (Note: Short term maintenance outages were not modeled as these are short in duration and fuel is typically not offloaded from the core.)

4

4

4

#### Fuel Assembly Data

Review of the discharged bundles currently residing in the spent fuel pool indicated that, prior to Cycle 13, all bundles were conservatively assigned a relative end-of-cycle power value of 1.0. Cycles 14, 15 and 16 assembly data contain calculated end-of-cycle assembly relative power values from 3-D core monitoring calculations. These calculated values were used to determine appropriate relative power values for future cycles. For Cycle 14, a weighted average end-of-cycle relative power of 0.74 was calculated. For Cycles 15 and 16 the weighted average relative end-of-cycle powers were 0.63 and 0.55, respectively. Thus, for future offloads, discharged assemblies were conservatively assumed to have relative power values of 0.8.

4

### Pool History and Cleanup Data

Pool history data (temperature, pH and reactive silica concentration) were added to the pool history file. In addition, letdowns to simulate mixing of the reactor cavity water with the bulk spent fuel pool water were added to the cleanup system file to coincide with the refueling outages occurring in October of 2006, 2008, 2010 and 2012.

### Assembly Shuffle and Dry Storage

Figure 3-1 shows the loading of the Peach Bottom 2 racks at the time of the last BADGER test. Freshly discharged bundles must be located such that "cold" bundles are on all four faces of adjacent cells. This requires some 1400 storage locations to accommodate a discharge batch of 276 fuel assemblies.

4

A major goal is to preserve Module 1 for staging reload fresh fuel as this module has seen the least severe service duty. Thus, Modules 3, 4, 5 and 12 were selected for placement of freshly discharged bundles. Figure 3-2 shows the projected loading pattern of the Peach Bottom spent fuel racks through 2013.

4

4

### 3.2 Future Projections

4

Using the input data and assumptions outlined in Section 3.1, the Peach Bottom RACKLIFE model was updated and executed through the dry storage campaign of 2012 through 2013. This served to identify the cells with the greatest panel boron carbide loss and absorbed dose. Figure 3-3 shows the percent boron carbide loss for the spent fuel racks in February 2006 at the time of the last BADGER test. The peak panel loss ([ ]) occurs in Module 15. This calculation used an escape coefficient of 1.0/day through February 2006 and 1.25/day beyond. The RACKLIFE model was executed iteratively by varying the "escape coefficient" until the predicted pool silica matched the measured pool silica. The escape coefficient is the rate, in units of cavity volumes (the volume of fluid in the rack cavities surrounding each Boraflex panel) per day that are exchanged with the bulk pool volume. An increase in the slope of the measured pool silica would indicate an increase in the escape coefficient is necessary. The physical basis for this is that as the Boraflex dissolves, the clearances for flow increase, reducing the pressure drop and increasing flow.

4

4

Figure 3-4 shows there is a fairly regionalized dose distribution throughout the pool. The majority of high dose panels (greater than  $1 \times 10^{10}$  rads) are located in a central region of the pool in front of the transfer canal. The panels with the highest dose are the south and west panels in cell XX65 of Module 15 with an integrated exposure of  $1.4 \times 10^{10}$  Rads.

Prior to the End-of-Cycle 16 (EOC16), there were vacant areas in Modules 10 and 11 as well as individually scattered vacant cells in Modules 6, 7, 8, 9, 14 and 15. It was decided that discharged bundles would reside in their "B.5.b" locations for 17 months (from discharge until the subsequent dry storage campaign) and then be moved to a vacant module. For the 2006 offload, B.5.b cell locations were vacated and resident bundles moved to Modules 10 and 11. In 2008, Module 11 was vacated and all bundles moved into dry storage casks. Bundles discharged in 2006 were subsequently moved to cells in Module 11. In 2010, bundles in Module 10 were "moved into dry storage" and B.5.b cell locations vacated with bundles discharged in 2008 relocated to module 10. The same process was repeated for the 2012 dry storage campaign, with bundles in Modules 14, 15 and part of Module 9 being placed into dry storage.

Figure 3-5 shows the distribution of panel boron carbide loss for the Peach Bottom spent fuel racks when the peak panel loss reaches 50 percent. The average panel boron carbide loss is [    ] percent with a standard deviation ( $1\sigma$ ) of [    ] percent.

4

Figure 3-6 shows the distribution of panel absorbed dose (Rads) for the Peach Bottom spent fuel racks corresponding to Figure 3-5. The average absorbed dose to all panels in the Peach Bottom spent fuel pool is  $7.5 \times 10^9$  Rads, while the maximum projected panel absorbed dose is  $2.5 \times 10^{10}$  Rads.

4



Figure 3-1: Occupied Cells in the Peach Bottom 2 Spent Fuel Storage Racks on February 26, 2006.



4

Figure 3-2: Projected Occupied Cells in the Peach Bottom 2 Spent Fuel Storage Racks through 2013.

Note: This figure reflects fuel moved into dry storage, as well as fuel shuffles to provide sufficient acceptable storage locations to accept freshly discharged fuel.

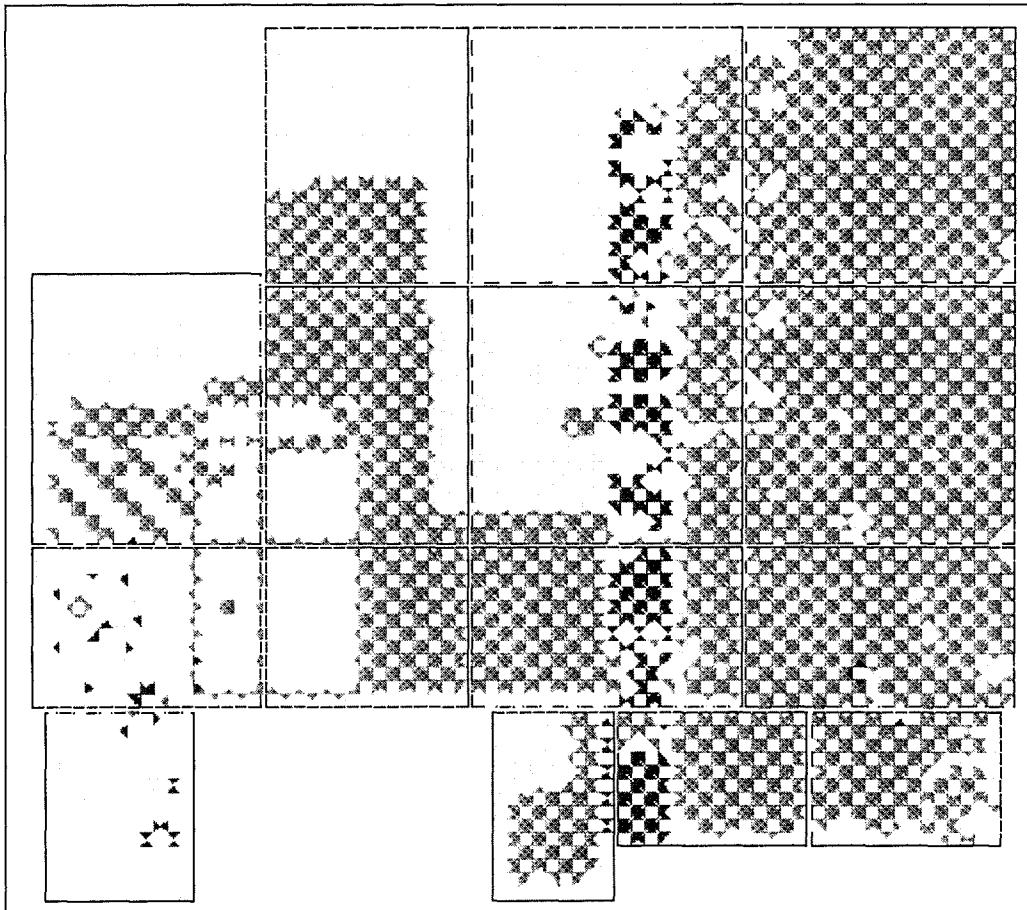


Figure 3-3: Predicted Boron Carbide Loss through February 26, 2006 in the Peach Bottom Spent Fuel Storage Racks

**Key:**

- Red:  $\geq 18\%$  loss
- Yellow:  $\geq 12\%$  loss but  $< 18\%$  loss
- Green:  $\geq 6\%$  loss but  $< 12\%$  loss
- Blue:  $\geq 3\%$  loss but  $< 6\%$  loss

NOTE: White cells are storage locations where the surrounding Boraflex panels are assigned to the face adjacent cells.

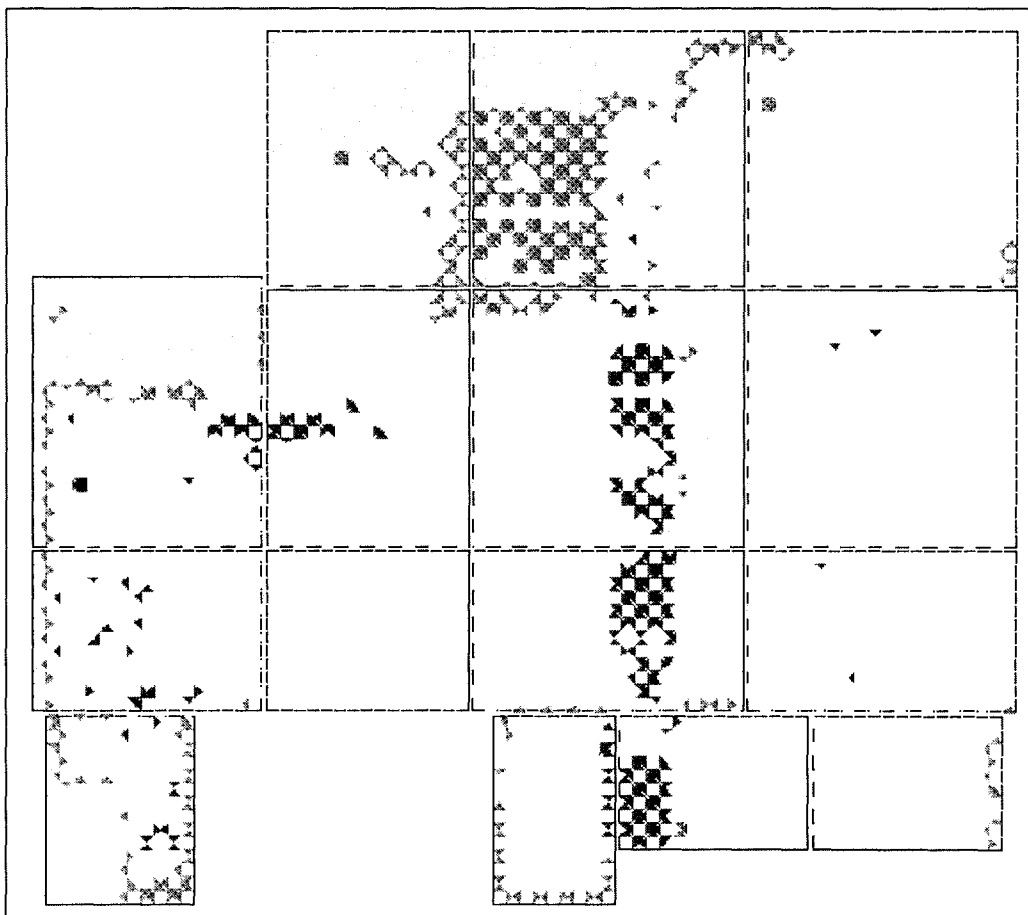


Figure 3-4: Panel Absorbed Dose through February 26, 2006 in the Peach Bottom Spent Fuel Storage Racks

**Key:**

- Red: Dose  $\geq 1 \times 10^{10}$  Rads
- Yellow  $\geq 2 \times 10^9$  Rads but  $< 1 \times 10^{10}$  Rads
- Green  $\geq 5 \times 10^8$  Rads but  $< 2 \times 10^9$  Rads
- Blue:  $< 5 \times 10^8$  Rads

NOTE: White cells are storage locations where the surrounding Boraflex panels are assigned to the face adjacent cells.



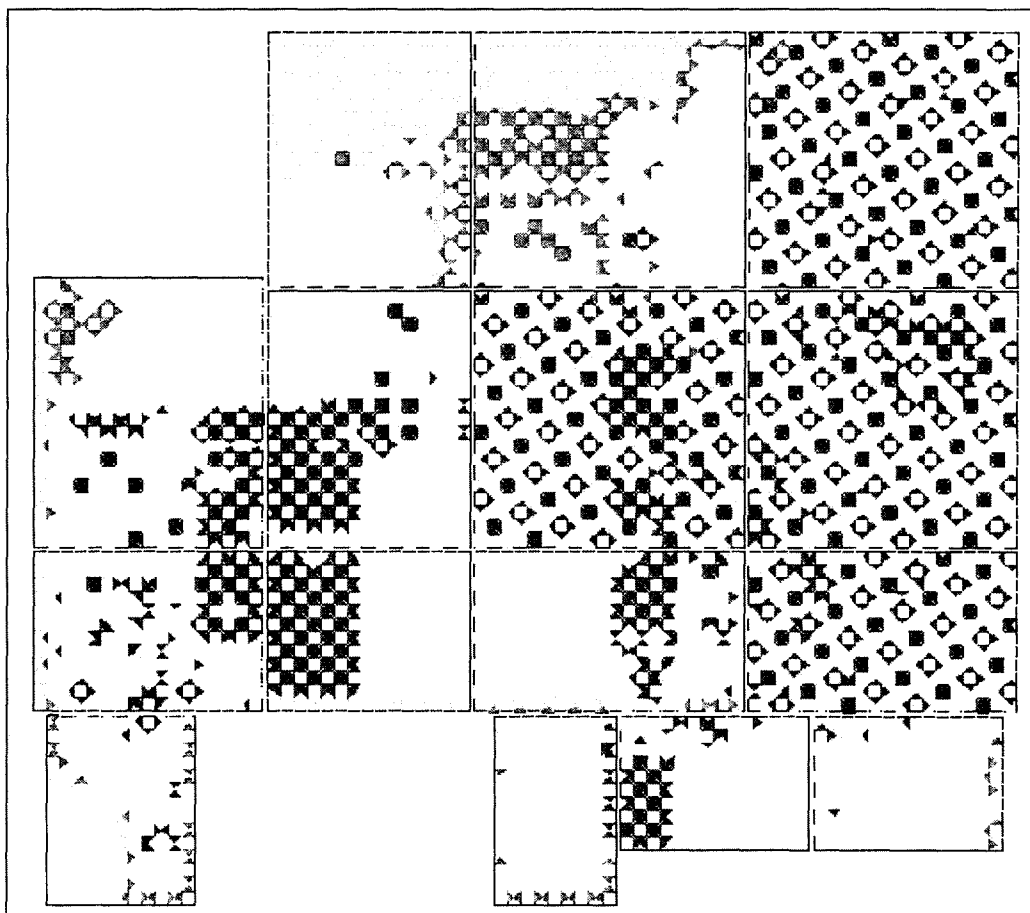
4

Figure 3-5: Predicted Boron Carbide Loss through 2013 in the Peach Bottom Spent Fuel Storage Racks

**Key:**

- Red:  $\geq 45\%$  loss but  $< 50\%$
- Yellow:  $\geq 30\%$  loss but  $< 45\%$  loss
- Green:  $\geq 15\%$  loss but  $< 30\%$  loss
- Blue:  $\geq 3\%$  loss but  $< 15\%$  loss

NOTE: White cells are storage locations where the surrounding Boraflex panels are assigned to the face adjacent cells.



4

Figure 3-6: Panel Absorbed Dose through 2013 in the Peach Bottom Spent Fuel Storage Racks

**Key:**

- Red: Dose  $\geq 1 \times 10^{10}$  Rads
- Yellow  $\geq 2 \times 10^9$  Rads but  $< 1 \times 10^{10}$  Rads
- Green  $\geq 5 \times 10^8$  Rads but  $< 2 \times 10^9$  Rads
- Blue:  $< 5 \times 10^8$  Rads

NOTE: White cells are storage locations where the surrounding Boraflex panels are assigned to the face adjacent cells.

## 4.0 The Reactivity Effects of Boraflex Degradation

### 4.1 Introduction

This section examines the reactivity effects of Boraflex panel degradation in the Peach Bottom spent fuel racks. Boraflex panel degradation can be divided into three modes, which are characterized by different degradation mechanisms, as described below.

#### 4.1.1 Uniform Dissolution

As described in Section 2.0, the Boraflex panels in the Peach Bottom spent fuel racks are contained in a "panel cavity" created between the [ ] inch thick stainless steel cell wall, and the [ ] inch thick stainless steel wrapper plate. The void volume of this panel cavity is filled with water that generally surrounds the Boraflex panel. The exchange of fluid between the bulk pool and the panel cavity (as measured by the "escape coefficient") results in a flow across the surfaces of the Boraflex panel as well as local flow paths in between the tack welds long the wrapper plate. This can lead to a relatively uniform dissolution of the amorphous silica from Boraflex panel surfaces along with local scallop regions and subsequent loss of absorber.

4

This mode of degradation increases the transmission of neutrons between assemblies in the spent fuel racks by decreasing the amount of intervening absorber. However, the remaining absorber still interposes between assemblies.

#### 4.1.2 Shrinkage, Including Gaps

Radiation induces crosslinking of the polymer matrix of Boraflex. This causes the material to shrink, reducing the volume of a Boraflex panel. While shrinkage reduces the volume of an interposing panel, shrinkage does not reduce the mass of interposing absorber, that is, the material undergoes densification as it shrinks.

Width and end shrinkage can “uncover” the active fuel, allowing direct neutron transport between assemblies without any intervening absorber. If a Boraflex panel is not allowed to shrink uniformly (e.g., it is mechanically restrained), gaps will develop. This can lead to direct neutron coupling between adjacent assemblies.

4

#### 4.1.3 Local Dissolution

The dissolution described in Section 4.1.1 above, is generally uniform. However, local non-uniformities in the panel, panel cavity, and cavity inlet/outlet geometry can accentuate dissolution locally. For example, a gap in a panel locally increases the cavity volume, which locally reduces the effects of wall friction on flow. This can increase local flow rates causing accelerated dissolution. As another example, a bend, bow, or creases in the stainless steel wrapper plates can provide result in orificed flow paths, allowing increased flow into or out of the panel cavity, thereby accelerating local degradation. These local effects can exhibit a positive feedback; they accelerate the local dissolution of Boraflex, which increases the local cavity volume. This in turn decreases wall friction losses, increasing local flow rates, further accelerating local Boraflex dissolution.

4

As suggested in the discussion for each mode of dissolution, each mode will affect the spent fuel pool reactivity differently. These synergistic reactivity effects may be strongly non-linear. Criticality safety calculations using highly bounding assumptions, (e.g., very large gaps all at the assembly mid-plane, complete dissolution of the Boraflex, etc.) lead to reactivity increases far in excess of the actual reactivity state of the spent fuel pool. On the other hand, the non-linear synergy necessitates a robust analysis of the degradation, in order to conservatively take some credit for the Boraflex that remains in the racks. This section of the report outlines a methodology for such a robust analysis.

#### 4.2 Methodology for Projecting Future Panel Conditions

The results of the latest BADGER test campaign at Peach Bottom Unit 2<sup>[8]</sup> were used to characterize the state of the Peach Bottom spent fuel rack Boraflex panels at the time of testing. The RACKLIFE projections (discussed in Section 3) were further used to

4

conservatively project the state of the panels to a future projected peak panel boron carbide uniform thinning loss of [ ] percent over the entire panel.

| 4

Algorithms were developed for randomly sampling panel local degradation features based on the BADGER data. The input to the algorithms are the panel absorbed dose and B<sub>4</sub>C loss predicted by RACKLIFE. The algorithms are based on random sampling from probability distributions of loss versus absorbed dose developed from the observed BADGER data. The use of normal and uniform random numbers in the algorithms account for variance observed between RACKLIFE predictions and BADGER observations and the random nature of local dissolution effects.

The Boraflex panel models developed represent degraded panels conservatively projected to a peak panel uniform thinning loss of [ ] percent. They consist of an array of rectangular blocks: four blocks across a panel to match the four detectors in BADGER, and each block two inches high to match the two-inch “window” in front of the BADGER detectors. Away from local areas of dissolution the blocks are as thick as a nominal panel of Boraflex. Each panel of Boraflex in the Peach Bottom spent fuel racks that was measured by BADGER was characterized using this system of blocks. Figure 4-1 is an example of a typical panel model. In Figure 4-1, the column heading “Elev” refers to the axial elevation of each block center. (The panel shown represents a [ ] inch panel; note that the panel is displayed top to bottom.) The columns are numbered to correspond to the four BADGER detectors and represent an area of the panel 1.23 inches wide by 2 inches high.

| 4

Integer values in Figure 4-1 represent an amount of gap in a block in thirds of an inch. Thus the row of “2”s on a red background indicates a two-thirds inch gap at an elevation of 43 inches. Cells in the panel model that are not colored are at a specified level of uniform loss. The values on blue backgrounds represent areas of local dissolution, quantified by the percent loss from the uniform loss condition. Some of the dissolution occurs around the gap, some near the end of the panel, and some independent of any other features of the panel. Yellow background represents dissolution in proximity to a

gap. Dissolution that occurs around a feature is assumed to extend into the feature.

For example, the [ ]% loss measured by detector 2 (column 2) at 131 inches is assumed to persist in the column 2 cell at 133 inches. In reality, BADGER would detect the additional loss if it was there, but this accounts for any uncertainty in an analyst's interpretation of how to allocate the loss. In the case of the gap at 43 inches, a loss of [ ]% is assumed under detectors 3 and 4 since this is (conservatively) the largest loss proximal to the gap.

In applying the panel models to the state of the Peach Bottom spent fuel racks in the future, the degree of conservatism used is best illustrated by the following examples.

4

#### Example 1: Loss Equivalence

The BADGER campaign at Peach Bottom Unit 2 in February 2006 measured the state of the Peach Bottom Unit 2 spent fuel rack Boraflex panels at that time. The RACKLIFE code was used to identify which panels in the Peach Bottom spent fuel racks had the highest absorbed dose and/or the highest predicted B<sub>4</sub>C loss. Measurements were performed on panels with a spectrum of dose and loss (in order to observe and quantify any trends with dose and loss), but with a strong bias toward the "worst" panels. Therefore, the panels that BADGER measured are typical of the worst panels in the pool. During the BADGER campaign in February 2006, 38 panels exhibited a measurable loss of boron carbide. The average loss from these 38 panels was [ ]%±[ ]%.

4

At the future point of 50 percent peak panel degradation, RACKLIFE predicts that the average loss for all panels in the racks is [ ]% ± [ ]%. These losses are comparable to what BADGER measured for the panels that actually exhibited a loss. For example, in predicting the condition of a 20% loss panel in the future, it is reasonable to assume that the condition would be equivalent to a 20% loss panel as measured by BADGER in 2006. If a 20% loss panel is not available, then the next higher loss panel measured is conservatively used. In this manner, projected panels in the future can be conservatively loss-equivalenced to panels measured by BADGER in 2006.

4

Example 2: Loss Extrapolation

At a future date when peak panel boron carbide loss reaches 50 percent, RACKLIFE predicts that the average loss in the racks is [ ] ± [ ]%. The average loss measured by BADGER (for all panels in 2006) was [ ]%. None of the panels exceeded the maximum loss of [ ]% predicted by RACKLIFE. Of the three modes of degradation described in Section 4.1, the first two, uniform dissolution and shrinkage, can be conservatively projected with a fair degree of confidence and precision. The degradation mechanisms are well understood and bounding models can be formulated. The third mode, local dissolution, however, is random in nature and is not as amenable to prediction.

4

For example, consider a typical local dissolution feature: a “scallop” in the side of the panel where higher levels of loss are observed. As illustrated below, suppose this takes the form of two 2” high by 1.23” wide rectangular cells along the left edge of the panel with 30% more loss than the uniform loss of the bulk panel. (The rectangular cells bound the actual size and shape of the scallop.)



The question is, more specifically now, what will this local dissolution feature look like in a panel that has undergone 1.5 times as much dissolution? Three distinct degradation scenarios can be considered: 1) the scallop increases in size by a factor of 1.5 (to three cells instead of two); 2) the scallop “deepens” by a factor of 1.5 (from 30% loss to 45% loss); or 3) the scallop remains the same and another one-cell scallop with 30% loss develops somewhere else on the panel. The actual scenario is likely a randomly weighted mixture of all three modes. To select a bounding degradation scenario is virtually impossible, since the reactivity effects of each scenario will depend on the elevation of the scallop, its proximity to other local dissolution features, gaps or end

4

shrinkage. The conservative approach used was to assume all three scenarios occur simultaneously on a cell-by-cell basis. As a conservative upper-bound, the next highest (worse) local dissolution pattern for the scallop was then selected.

Using the panel projections described above, the methodology described in section 4.3 was developed for simulating the reactivity effects of Boraflex panel degradation.

#### 4.3 Methodology for Assessing the Reactivity Effects of Boraflex Degradation

The methodology described below was applied to the Peach Bottom spent fuel racks with each cell containing a GNF2 bundle. For clarity, the description below will generally refer to the racks generically.

4

The SCALE code package (described in Section 5.2) was used to calculate  $k_{\text{eff}}$  for the racks. For the reactivity equivalence model, the Boraflex was assumed to be at its nominal thickness and  $^{10}\text{B}$  loading. In addition, a conservatively bounding 4.1% width shrinkage was also applied. This bounding shrinkage is based on both analytical and experimental analyses<sup>[2]</sup> and has been confirmed by a large number of proprietary laboratory studies and field observations. Recall from Section 4.1 that thickness shrinkage is effectively offset by densification and so need not be accounted for. As described in Section 4.1, the effects of axial shrinkage manifest themselves as both end shrinkage and gapping. Measuring the amount of shrinkage-induced gapping is complicated by the fact that local dissolution can increase the apparent size of a gap.

Further, BADGER may miss gaps that are less than 1/3<sup>rd</sup> inch. To account for the axial shrinkage with the possibility that some gaps may have been missed, it is conservatively assumed that every panel has an undetected 4.1% axial shrinkage in the form of 1/3<sup>rd</sup> inch gaps uniformly distributed up the panel. The reactivity effect of this assumption is shown in Table 4-1. These assumptions result in a higher than nominal reactivity model, which conservatively increases the reactivity effects of Boraflex loss.

4

The Boraflex thickness in the base model was then uniformly decreased in 10% increments to observe the reactivity effects of uniform dissolution. The results were used to develop a relationship between uniform thinning and an increase in  $k_{\text{eff}}$  for reactivity equivalencing between pure uniform thinning and the actual degraded condition of the Boraflex. The results for bounding thinning amounts that bracket the target value [ ]% are shown in Table 4-2. 4

Next, a verified and validated Fortran program was used to modify the base case, so that every panel in a given array of rack cells could be modeled independently. The algorithms described in Section 4.2 were used to create panel models as described in that section for each panel in the array. For this analysis, a [ ] array of cells was modeled, thus, a total of [ ] panels are generated by the algorithm according to the dose and loss predicted by RACKLIFE for each panel. The [ ] array is repeated periodically in the x and y direction. These degraded models of Boraflex panels are incorporated into a KENO model to simulate the conditions of the module when maximum peak panel uniform thinning is [ ]%. This case is used to calculate a single estimate of the reactivity effect of Boraflex panel degradation in the Peach Bottom Unit 2 spent fuel rack modules. The salient features of the model are:

- Each configuration contains a [ ] array of storage cells
- Each cell contains two associated panels of Boraflex ([ ]=32 panels)
- Periodic boundary conditions are applied
- Each cell contains a design basis GNF2 fuel bundle
- Each Boraflex panel contains local dissolution scallops, gaps and shrinkage in addition to [ ] percent uniform thinning
- The fuel is assumed to be 145.24 inches and at the peak reactivity. The Peach Bottom fuel is 150 inches (with 6-inch natural uranium ends. The [ ]-inch Boraflex normally exceeds the enriched region by 4 inches.

In executing the case, a total of 30 million neutrons were tracked over 3000 generations. Fifty generations were skipped to ensure convergence of the source distribution. The large number of neutrons was used to ensure that there was adequate

sampling of all of the degradation features of all of the panels in the model. As per standard practice, plots and statistics of the evolution of  $k_{eff}$  by generation were inspected and calculated to provide confidence that no sampling instabilities were being encountered.

As described in Section 4.2, the Boraflex panels generated for the model were based on a sequence of random numbers, so that each panel model is a random model with an expected value defined by the BADGER measurements plus a random variance. Consequently, the single estimate case described above could be randomly higher or lower than the actual condition of the panel being modeled. Therefore a total of [ ] independent and randomly distributed cases were created using the Fortran program. These cases resulted in a distribution of calculated reactivity effects. The 95<sup>th</sup> percentile of this reactivity effects distribution, at 95% confidence, can be used to bound the reactivity effects of degraded Boraflex panels in the array of cells being considered.

Figure 4-2 shows one example of this distribution as points in a cumulative distribution with the Monte Carlo statistical uncertainty, as shown by the error bars. The line in Figure 4-2 is a cumulative normal distribution with a mean and variance from the [ ] samples. In every distribution calculated, the data passed the Anderson-Darling and Cramér-von Mises tests for normality; thus, one-sided normal distribution statistical tolerance factors are valid for calculating bounding 95<sup>th</sup> percentile eigenvalues at 95% confidence. Figure 4-2 shows that [ ] samples are sufficient to bracket the 95<sup>th</sup> percentile and to look for any potential non-normal behavior in the tails. No non-normal behavior was observed.

#### 4.4 Results

Table 4-3 summarizes the reactivity effects in the Peach Bottom spent fuel racks. The RACKLIFE predicted loss, as a uniform thinning loss, is shown in column 1. The RACKLIFE code does not distinguish between uniform loss and local dissolution losses. The reactivity effect in column 2 is the 95<sup>th</sup> percentile effect at 95% confidence and includes the effects of uniform dissolution, local dissolution, and gaps.

4

Table 4-2 was used to interpolate the equivalent amount of uniform thinning loss that will yield the same reactivity effect as the 95/95 effect above. The results are shown in column 3. The value of [ ]% for the equivalent loss in the racks is a conservative over-estimate of the actual equivalent loss. Most of the panels measured by BADGER in 2006 had very low losses compared to the losses predicted for the population of panels. Thus, in equivalencing observed panel losses with predicted losses, a large amount of conservatism was introduced for the low loss panels.

| 4

Column 4 shows the conservative amount of uniform thinning loss that will be assumed in subsequent analyses. The many conservatisms used to arrive at these numbers provides confidence that these losses will bound the state of the Peach Bottom spent fuel racks.

| 4

**Table 4-1: Conservative Reactivity Effects of Cracks Undetected by BADGER**

--	--

| 4



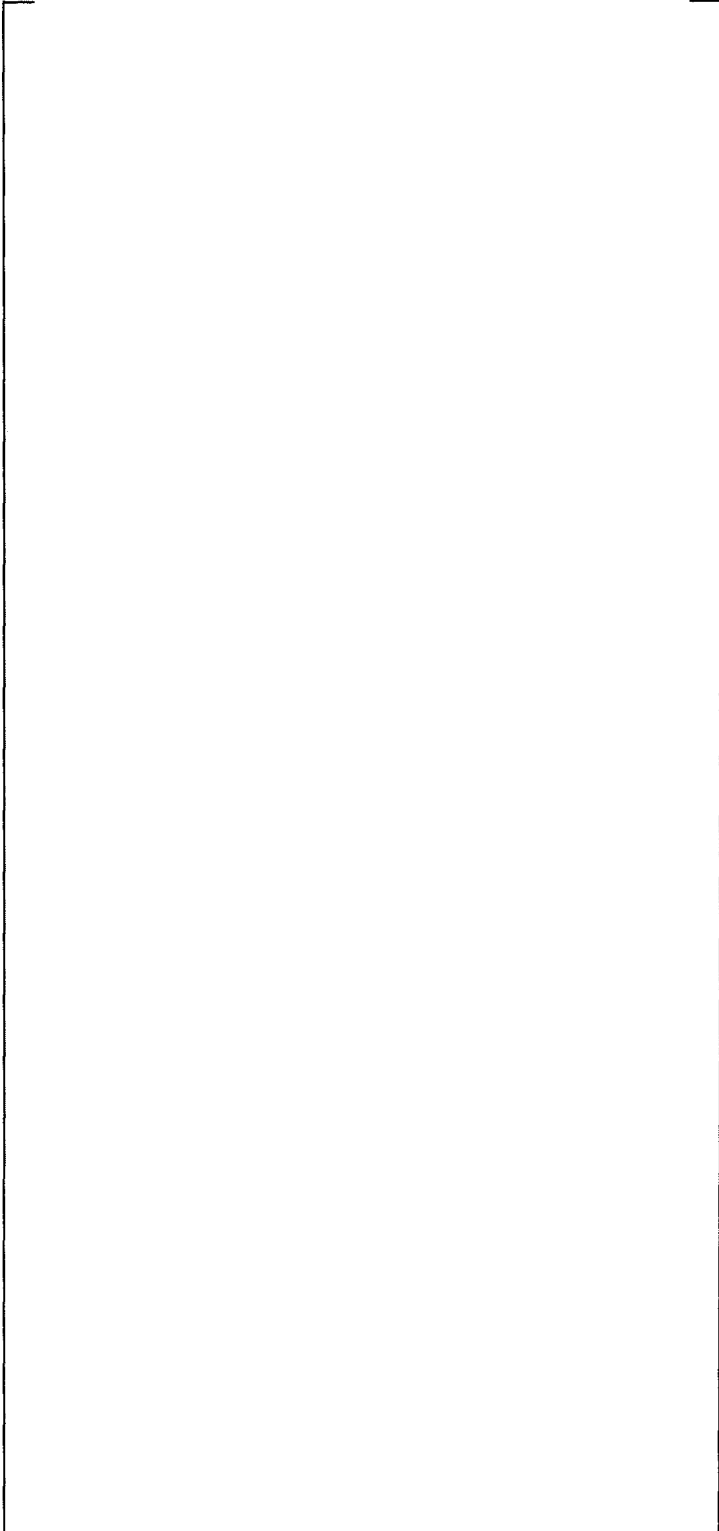


Figure 4-1: Typical Model of a Peach Bottom Unit 2 Boraflex Panel



Figure 4-2: Sample Distribution of Panel Degradation Reactivity Effects

## 5.0 Results of the Criticality Analysis

The criticality analyses and evaluations described in this report demonstrate that the  $k_{\text{eff}}$  of the Peach Bottom spent fuel racks is less than or equal to 0.95 when loaded with the most reactive (GNF2) fuel type under the most reactive conditions, assuming a maximum projected boron carbide loss of [ ]% uniform thinning over the entire length of the Boraflex panels. The maximum calculated reactivity ( $k_{\text{eff}}$ ) when adjusted for computer code biases, fuel and rack manufacturing tolerances and methodology/calculational uncertainties (combined using the root-mean-square method) will be less than or equal to 0.95 with a 95% probability at a 95% confidence level.

4

### 5.1 Design Basis and Design Criteria

All analyses and evaluations have been conducted in accordance with the following codes, standards and regulations as they apply to spent fuel storage facilities:

- American Nuclear Society, American National Standard Design Requirements for Light Water Reactor Spent Fuel Storage Facilities at Nuclear Power Plants, ANSI/ANS-57.2-1983. October 7, 1983. (Withdrawn in 1993. However, this standard is endorsed by NUREG-0800, Section 9.1.1.)
- Nuclear Regulatory Commission, Letter to All Power Reactor Licensees from B. K. Grimes. *OT Position for Review and Acceptance of Spent Fuel Storage and Handling Applications*. April 14, 1978, as amended by letter dated January 18, 1979.
- Nuclear Regulatory Commission, memorandum from Laurence Kopp to Timothy Collins. *Guidance on the Regulatory Requirements for Criticality Analysis of Fuel Storage at Light-Water Reactor Power Plants*. August 19, 1998.
- USNRC Standard Review Plan, NUREG-0800, *Standard Review Plan for the Review of Safety Analysis Reports for Nuclear Power Plants*, Section 9.1.1, "Criticality Safety of Fresh and Spent Fuel Storage Handling," March 2007. (S.E.P. 9.1.1 endorses ANSI/ANS-57.1, 57.2 and 57.3, however only 57.2 applies to spent fuel pool criticality.)

4

4

- NUREG/CR-6698, *Guide for Validation of Criticality Safety Computational Methodology*, Nuclear Regulatory Commission, January 2001.
- ANSI/ANS 8.17-1984, *Criticality Safety Criteria for the Handling, Storage and Transportation of LWR Fuel Outside Reactors*, American Nuclear Society, January 1984 (Withdrawn 2004).
- 10 CR 50.68, Subsection B.4, *Criticality Accident Requirements*.

4

It is noted that the above USNRC and ANS documents refer to the requirement that the maximum effective neutron multiplication factor ( $k_{\text{eff}}$ ) is to be less than or equal to 0.95. In demonstrating that this requirement is satisfied, the analyses herein of the reference (nominal dimensions) case fuel/rack configurations are based on an infinite repeating array in all directions.

4

## 5.2 Analytical Methods and Assumptions

This analysis utilizes the stochastic three-dimensional Monte Carlo code KENO V.a<sup>[14]</sup> and the two-dimensional deterministic code CASMO-4<sup>[15]</sup> to compute the reactivity effects due to degraded Boraflex. The CASMO code yields a deterministic solution to the neutron transport equation, which is useful for precisely computing incremental reactivity changes. The stochastic nature of the Monte Carlo solution in KENO means that statistical tolerance factors at 95% probability with 95% confidence must be applied to the solution. On the other hand, CASMO is limited to two-dimensional (axially uniform) single cell (infinitely reflected) models, while KENO provides robust three-dimensional modeling capability. Thus, KENO is used when axial effects are important (e.g., axially distributed gaps), or when lateral non-uniformities are present (e.g., checkerboard loading).

4

KENO V.a is a module in SCALE 5.0, a collection of computer codes and cross section libraries used to perform criticality safety analyses for licensing evaluations. KENO solves the three-dimensional Boltzmann transport equation for neutron-multiplying systems. The collection also contains BONAMI-S to prepare problem-specific master

cross section libraries and to make unresolved resonance region self-shielding corrections for nuclides with Bondarenko data. NITAWL-II is used to prepare a working cross section library with resolved resonance region self-shielding corrections using the Nordheim integral treatment. These modules are invoked automatically by using the CSAS25 analysis sequence in SCALE 5.0.

4

CASMO-4 is a two-dimensional multigroup transport theory code for fuel assembly burnup analysis in-core or in typical fuel storage racks. CASMO is a cell code in which infinitely repeating arrays of fuel assemblies and/or fuel racks are modeled.

These codes have been verified by others for use in spent fuel rack design evaluations by using them to model critical experiments. NETCO has validated their use for spent fuel rack criticality analyses. The results of the validation effort are included in this report as Appendix A. The calculated  $k_{\text{eff}}$  was compared to the critical condition ( $k_{\text{eff}} = 1.0$ ) to determine the bias in the calculated values.

4

In all SCALE/KENO calculations, the 238-energy group ENDF/B-V criticality safety cross section library<sup>[21]</sup> was used. The resulting benchmark bias and (95/95) bias uncertainty in the SCALE codes was calculated to be [ ] via non-parametric methods. In all CASMO-4 calculations, the 70-energy group neutron library<sup>[15]</sup> was used. The resulting bias and ( $1\sigma$ ) bias uncertainty in the CASMO-4 code was calculated to be [ ]. The 95/95 statistical one-sided tolerance factor for CASMO ( $n=24$  benchmarks) is  $K \approx 2.309$ .<sup>[22]</sup>

4

The depletion characteristics of GNF2 bundle ( $k_x$  versus burnup) in both the core geometry and fuel rack geometry have been assessed with CASMO-4 to determine the burnup resulting in peak bundle reactivity ( $k_x$ ). In these calculations the fuel bundle is depleted at hot full power conditions (0%, 40% and 70% void) in-core geometry using CASMO-4. At specified burnup steps the bundle is brought to the cold zero power condition (no Xenon) and modeled in the rack geometry. Subsequently, the bundle is subjected to additional burnup in the hot full power condition in-core geometry and the process repeated.

4

The design point for the Peach Bottom fuel racks is taken at the burnup corresponding to peak reactivity of the  $\text{Gd}_2\text{O}_3$  bearing maximum reactivity bundle. Appendix B contains a summary of the peak reactivities of the GNF2 design basis bundle lattices

4

and older fuel types stored in the Peach Bottom spent fuel pools. The peak lattices for the 7x7, 8x8, 9x9 and older 10x10 fuel types were identified and provided by GNF<sup>[11]</sup>. The lattices were then evaluated using CASMO-4 to determine the peak in-rack reactivity lattice (Vanished1).

4

To assure that the actual fuel/rack reactivity is always less than the calculated maximum reactivity, the following conservative assumptions have been applied to the analyses:

1. The fuel assembly design parameters for these analyses are based on the most reactive 10 x 10 fuel types.
2. The maximum fuel enrichment is [ ] w/o U<sup>235</sup> with gadolinia and is assumed to be uniform throughout the bundle. The assumption of uniform enrichment results in a higher reactivity than would the distributed enrichment, which actually exists in the bundles. Since BWR fuel lattices must meet margins to critical power and linear heat generation limits, as-fabricated lattices will always have non-uniform enrichment.
3. The fuel bundle includes a coolant flow channel in the rack as this condition results in the highest reactivity. The effect of storage of a fuel assembly without a channel was analyzed and found to result in a less reactive condition than storage of the fuel assembly with a channel. This is a result of the storage rack system being over moderated.
4. The moderator is assumed to be demineralized water at full water density (1.0 gm/cm<sup>3</sup>). This bounds the water density down to a bounding minimum fuel and rack temperature of 4°C.
5. The array is an infinite repeating array in the x and y directions and infinitely long in the z direction.
6. All available storage locations are loaded with bundles of maximum reactivity (GNF2 Vanished1 lattice).
7. No credit is taken for neutron absorption in the fuel assembly grid spacers. This is conservative in that it adds pure unborated water to the region near the fuel pins. The region around the fuel pins is undermoderated and therefore adding water will increase reactivity.
8. No credit is taken for any natural uranium or reduced enrichment axial blankets. Neutron absorption in end fittings and tie plates is also neglected.
9. Boraflex is assumed to be uniformly at [ ]% nominal thickness (i.e., [ ]% uniform thinning loss) and at the minimum width. Tolerances were

4

4

4

4

4

conservatively evaluated at [ ]% uniform thinning. This is conservative as additional Boraflex thinning increases reactivity.

10. The active fuel length is 145.24 inches. While the reference case is infinite in all directions, the reactivity effects of Boraflex degradation presented in Section 4 assumed that the fuel extended beyond the [ ]-inch Boraflex panel length (including shrinkage). This reactivity effect is included in the equivalent panel thinning used in the reference model.

4

Beginning-of-life (BOL) fuel dimensions and material compositions (for non-fuel materials) have been assumed in this analysis. Fuel exposure results in channel growth (bulge), grid spacer growth (increased rod-to-rod pitch) and buildup of activated corrosion and wear products (CRUD). Channel growth is addressed below in Section 5.3.3.

As fuel is irradiated, a small amount of x-y axis grid spacer growth is expected. However, its effect on reactivity (increased rod-to-rod pitch) is considered to be negligible, and conservatively bounded by the BOL manufacturing rod-to-rod dimensional tolerances at the time the fuel bundle has reached an exposure corresponding to peak reactivity. Additionally, this analysis has conservatively neglected to include the negative reactivity introduced by the presence of grid spacers (strong neutron absorbing material) in the analysis, which offsets the effects of small increases in reactivity due to increasing rod-to-rod pitch. CRUD buildup is conservatively neglected because most of these compounds have higher neutron absorption cross sections than water, thereby reducing fuel bundle reactivity.

Based on the analyses described subsequently the maximum  $k_{eff}$  of the fuel/rack configuration at a 95% probability with a 95% confidence level is calculated as:

$$k_{eff} = k_{ref} + \Delta k_{bias} + \sqrt{\sum_{n=1}^{16} \Delta k_n^2}$$

where

$$\begin{aligned} k_{ref} &= \text{Nominal } k_{eff} \text{ adjusted for depletion effects} \\ \Delta k_{bias} &= \Delta k_{method} + \Delta k_{self-shielding} + \Delta k_{undetected cracks} + \Delta k_{Leakage} \\ &\quad + \Delta k_{geometry} + \Delta k_{accidents} \end{aligned}$$

Tolerances and Uncertainties:

- $\Delta k_1$  = UO<sub>2</sub> enrichment tolerance
- $\Delta k_2$  = Fuel stack density tolerance
- $\Delta k_3$  = Gd<sub>2</sub>O<sub>3</sub> loading tolerance
- $\Delta k_4$  = Pellet diameter tolerance
- $\Delta k_5$  = Clad thickness tolerance
- $\Delta k_6$  = Rod-to-Rod spacing
- $\Delta k_7$  = Storage cell pitch tolerance
- $\Delta k_8$  = Storage cell wall thickness tolerance
- $\Delta k_9$  = Boraflex B-10 loading tolerance
- $\Delta k_{10}$  = Asymmetric assembly position tolerance
- $\Delta k_{11}$  = Channel bulge effect
- $\Delta k_{12}$  = KENO V.a Methodology bias uncertainty (95/95)
- $\Delta k_{13}$  = CASMO Methodology bias uncertainty (95/95)
- $\Delta k_{14}$  = KENO V.a calculation uncertainty (95/95)
- $\Delta k_{15}$  = Burnup uncertainty
- $\Delta k_{16}$  = BADGER Measurement uncertainty ( $2\sigma$ )

4

The tolerances are statistically independent and can be combined in the root-mean-square manner.

### 5.3 Calculated Results

#### 5.3.1 Reference Eigenvalue Calculations

The fuel racks have been analyzed for GNF2 fuel with a maximum average planar enrichment of [ ] w/o U-235 and a minimum of [ ] gadolinia rods with a minimum loading of [ ] w/o Gd<sub>2</sub>O<sub>3</sub> and [ ] gadolinia rod with a minimum loading of [ ] w/o Gd<sub>2</sub>O<sub>3</sub>. The fuel design parameters for the GNF2 fuel assembly are summarized in Table 5-1.

4

The reactivity effects of combined local dissolution, shrinkage induced gaps and uniform thinning are equivalent in reactivity to a uniform panel thinning of [ ]%. It was conservatively assumed that the panel thickness was at [ ]% of the nominal thickness ([ ]). This effect is modeled in the base eigenvalue ( $k_{ref}$ ).

4

CASMO-4 was applied to compute the reactivity of the in-rack peak reactive GNF2 Vanished1 lattice, listed above. Figure 5-1 contains a plot of rack  $k_{\infty}$  versus burnup for the in-rack peak reactive GNF2 Vanished1 fuel lattice depleted at hot full power conditions as specified in Reference 11 at the 0% void condition. This was higher in reactivity relative to depletion at higher (40 and 70 percent) void fractions. As shown in

4

this figure the GNF2 fuel bundle with  $Gd_2O_3$  has an in-rack, bias-corrected peak reactivity of  $k_{\infty} = [ \quad ]$  which occurs at  $[ \quad ]$  GWD/MTU.

This bias-corrected in-rack peak reactivity,  $k_{\infty} = [ \quad ]$ , was calculated using CASMO. As such, the geometric limitations of this infinite array two-dimensional criticality code did not permit explicit modeling of the geometric asymmetries of the Peach Bottom spent fuel racks. A KENO V.a model which mirrored the CASMO-4 geometry was created. The model is infinite in the x,y,z directions with no gadolinia at a reactivity fresh fuel enrichment (REFFE) that has been determined to be equivalent to the reactivity of the same bundle depleted by CASMO-4 up to the burn-up at peak reactivity (see Figure 5-1). Using this KENO V.a model of the CASMO-4 geometry, KENO V.a was executed several times while iterating on  $U^{235}$  enrichment to determine the REFFE that resulted in a bias-corrected, in-rack  $k_{\infty} = [ \quad ]$ . This corresponds to an REFFE of  $[ \quad ]$  weight percent  $U^{235}$ .

4  
4

#### Cross-Section Bias

To further illustrate the fidelity between CASMO and KENO V.a calculations, a zero burn-up comparison between the CASMO-4 rack model and a KENO V.a model of the CASMO geometry was performed. This served to identify any differences in reactivity due to different cross section sets of the two codes. The difference (CASMO-KENO) ( $\Delta k_{x-secs}$ ) in respective  $k_{\infty}$  values was determined to be negative  $[ \quad ]$ , however, this is conservatively assumed to be zero.

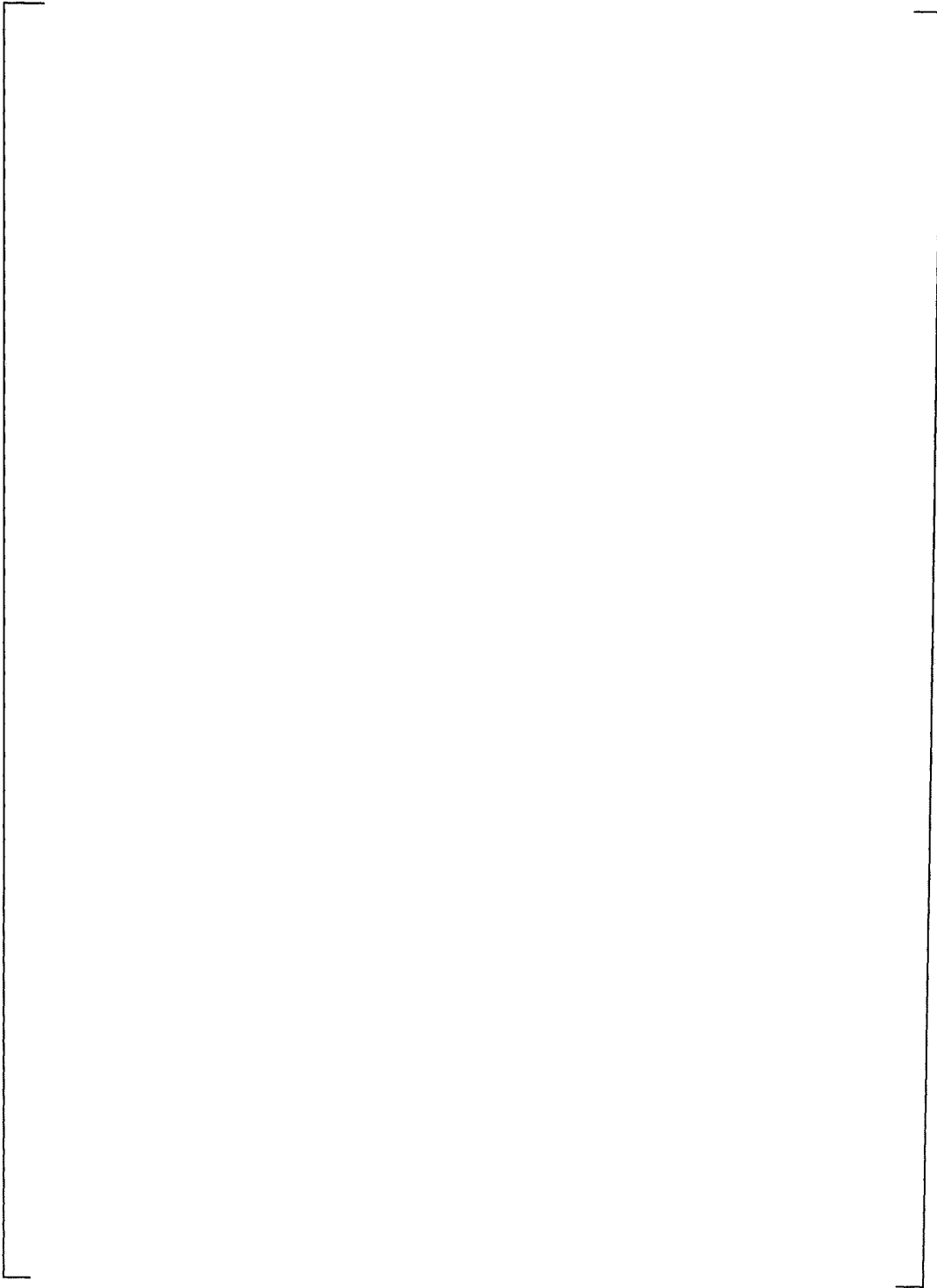
4

#### CASMO/KENO Geometry Bias

CASMO is somewhat limited in its ability to model asymmetric fuel rack designs. The Peach Bottom spent fuel racks have slight asymmetries due to wrapper plates and because every other cell is formed by the walls of the nearest neighbors. To quantify the geometric effects of the CASMO simplified geometry, a KENO V.a model of the explicit Peach Bottom spent fuel racks was created. This model was used to approximate the difference in  $k_{\infty}$  value so calculated with the  $k_{\infty}$  value calculated using the CASMO-4 geometry. The calculated difference (CASMO-KENO) was  $\Delta k_{geom} = [ \quad ]$ . This value of geometry bias was assumed to be zero and shows that the CASMO-4 calculated in-rack value of  $k_{\infty}$ , to be conservative by at least  $0.003\Delta k$ .

4  
4

**Table 5-1**  
**GNF2 Fuel Assembly Description**  
**Peach Bottom Nuclear Generating Station**



| 4

| 4

| 4



4

Figure 5-1: Bias-Corrected, In-Rack<sup>+</sup> Reactivity versus Burnup\* for the GNF2 Vanished1 Fuel Type in the Peach Bottom Spent Fuel Storage Racks.

\* (0% void)

<sup>+</sup>20°C, density<sub>h2o</sub> = 1.0 gm/cc

5.3.2 CASMO-4 and KENO V.a Reactivity Calculations in-Core and in-Rack Geometries

As a check of the two independent methods used for these analyses, the reactivity of the limiting GNF2 design basis lattice in the standard core geometry at cold conditions (20°C) have been calculated with both KENO V.a and CASMO-4 at zero burnup. Table 5-2 contains the core  $k_{\infty}$  for the GNF2 bundles with and without Gd<sub>2</sub>O<sub>3</sub> rods. The reported values include model biases, which have been determined via benchmark calculations. These benchmark biases are [ ] and [ ] for KENO V.a and CASMO-4, respectively. Table 5-3 contains a similar comparison of the Peach Bottom in-rack  $k_{\infty}$  as calculated with KENO V.a and CASMO-4.

4

4

**Table 5-2**

**CASMO-4/KENO V.a Reactivity Comparison in Core Geometry:**

**GNF2 Vanished 1 Lattice @ [ ] w/o U-235 ([ ]% T.D.), Zero Burnup, 20°C**

[

]

4

**Table 5-3**

**CASMO-4/KENO V.a Reactivity Comparison in Rack Geometry:**

**GNF2 Vanished 1 Lattice @ [ ] w/o U-235 ([ ]% T.D.), Zero Burnup, 20°C**

[

]

4

In addition, the  $k_{\infty}$  at peak reactivity in the Standard Cold-Core Geometry (SCCG) as calculated by CASMO-4 was bias corrected [      ].

| 4

The small differences in the eigenvalues are likely attributable to small differences in cross sections. This comparison serves to validate the use of these calculational methods.

| 4

### 5.3.3 Effect of Tolerances and Uncertainties

#### Tolerances and Calculational Uncertainties

To evaluate the reactivity effects of fuel and rack manufacturing tolerances, CASMO-4 and KENO V.a perturbation calculations were performed. The most reactive GNF2 fuel bundle (with  $Gd_2O_3$ ) at a burnup of [ ] GWD/MTU was used. The following tolerance and uncertainty components are addressed, based upon 60% uniform thinning:

U-235 Enrichment ( $\Delta k_1$ ): The enrichment tolerance of  $\pm$  [ ] w/o U-235 variation about the nominal reference value of [ ] w/o U-235 was considered<sup>[11]</sup>.

Fuel Stack Density( $\Delta k_2$ ): An upper tolerance level of  $\pm 1.30\%$  about the nominal reference theoretical density of [ ]%<sup>[11]</sup> was assumed.

Pellet Dishing: The pellets were assumed to be undished. This is a conservative assumption in that it maximizes the U-235 loading per axial centimeter of the fuel stack. No sensitivity analyses were completed with respect to the variations in the pellet dishing factor.

Gd<sub>2</sub>O<sub>3</sub> Loading( $\Delta k_3$ ): The tolerance of  $\pm$ [ ]%<sup>[11]</sup> (relative) has been assumed.

Pellet Diameter( $\Delta k_4$ ): A manufacturing tolerance of  $\pm$  [ ] cm was considered<sup>[11]</sup>.

Clad Thickness( $\Delta k_5$ ): A manufacturing tolerance of  $\pm$  [ ] cm was considered<sup>[11]</sup>.

Rod-to-Rod Spacing( $\Delta k_6$ ): A bounding tolerance of  $\pm$  [ ] cm was considered. This was based on a bounding outer spacer tolerance of  $\pm$  [ ] cm per discussions with GNF.

Storage Cell Pitch( $\Delta k_7$ ): The manufacturing tolerance of  $\pm$  [ ] inches for the variations in center-to-center spacing was used. The tolerance on the storage cell inside dimension is inherently included in the storage cell pitch tolerance.

Storage Cell Wall Thickness( $\Delta k_8$ ): A stainless steel sheet tolerance of  $\pm$ [ ] inches consistent with previous analyses was used.

Boraflex Width: The Boraflex material was modeled at the minimum width tolerance.

Boraflex Loading( $\Delta k_9$ ): A manufacturing tolerance of  $\pm$  [ ] gm B<sup>10</sup>/cm<sup>2</sup> was used based on a review of Boraflex batch records<sup>[6]</sup>.

4

Boraflex Thickness: As described in Section 4.3, the reactivity effect due to density increase from shrinkage offsets the small effect of a reduction in thickness tolerance.

Asymmetric Assembly Location( $\Delta k_{10}$ ): The reference CASMO reactivity calculations are based on a model with each bundle symmetrically positioned in each storage cell. The effect of four adjacent assemblies with minimum separation distance has been considered and has a negative effect on reactivity. Additionally, simple rotation of the assemblies does not produce statistically significant differences in the reference eigenvalue as calculated by KENO. The all-centered condition maximizes neutron coupling between adjacent storage cells and therefore results in the highest reactivity.

Channel Bulge( $\Delta k_{11}$ ): The effect of channel bulge was analyzed to determine its impact or reactivity relative to the reference case model of an assembly with a channel at nominal dimensions. This perturbation yielded a negative reactivity effect of due to channel bulge.

Methodology Uncertainty( $\Delta k_{12,13}$ ): The 95% probability/95% confidence level KENO V.a uncertainty of [ ] and the 95% probability/95% confidence level CASMO-4 uncertainty of [ ] have been determined from benchmark calculations (see Appendix A). The CASMO-4 uncertainty contains the one-sided tolerance factor as discussed in Section 5.2. The KENO V.a uncertainty was determined via non-parametric methods. The result of the CASMO uncertainty on reactivity is included in Table 5-4. The KENO V.a uncertainty is included for information only, and need not be included in the calculation of  $k_{eff}$ , as  $k_{ref}$  was determined using CASMO-4.

KENO V.a Calculation Uncertainty( $\Delta k_{14}$ ): This is the calculation uncertainty (standard deviation) for a single calculation (typically  $<0.0003$ ) with a one-sided tolerance factor of  $\kappa = 1.7$  for 3000 neutron generations.

#### Burnup Uncertainty ( $\Delta k_{15}$ )

Critical experiment data are generally not available for spent fuel and accordingly, some judgment must be used to assess uncertainties introduced by the depletion calculations. CASMO-4 and the 70-group cross section library used for these analyses has been used extensively to generate bundle average cross sections for core follow calculations and reload fuel design in both BWRs and PWRs. Any significant error in those depletion calculations would be detectable either by in-core instrumentation measurements of core power distributions or cycle energy output or both. Significant deviations between the predicted and actual fuel cycle lengths and core power distributions using CASMO-4 generated cross sections are not observed.

4

For the purpose of assessing the effects of uncertainties introduced by depletion calculations, it is useful to estimate the magnitude of depletion uncertainties in  $k_{\infty}$  and compare this uncertainty with margins inherent in the present calculation. Reference 23 suggests a reactivity uncertainty equivalent to 5 percent of the reactivity decrement from 0 burnup to the burnup of interest. For this analysis, the reactivity increase from 0 burnup to peak reactivity (16GWD/mtu) is [ ]  $\Delta k$ . The resulting burnup uncertainty would be [ ]  $\Delta k$ . For the limiting GNF2 bundle at [ ] GWD/MTU, the uncertainty introduced by depletion is included in Table 5-4.

4

BADGER Measurement Uncertainty ( $\Delta k_{16}$ )

The standard deviation in the areal density measurements for the 38 panels that exhibited a boron carbide loss in 2006 was [ ]% ( $1\sigma$ ). This reactivity effect ( $\Delta k_{16}$ ) of [ ]% uniform thinning is [ ]. This was added as a  $2\sigma$  uncertainty in Table 5-4.

4

Self-Shielding of Discrete Absorber Particle Size ( $\Delta k_{\text{self shield}}$ )

4

The absorber discrete particle self-shielding bias accounts for the fact that Boraflex is made from discrete boron carbide particles and thus is not a homogeneous distribution of absorber particles. The effect of discrete particle self-shielding was based on a typical particle distribution size for boron carbide used in Boraflex. The analysis indicated that an equivalent homogenous density of [ ]% of the nominal B-10 density would yield a reactivity effect equivalent to an absorber panel containing discrete absorber particles<sup>[25]</sup>.

4

To account for the absorber discrete particle self-shielding, two KENO calculations were evaluated. The first (the reference configuration) assumed a Boraflex B-10 loading with infinitely small, uniform particle distribution, at 100% of the material design basis. The second assumed a Boraflex B-10 loading with infinitely small, uniform particle distribution, at [ ]% of the material design basis. The difference between these two calculations represents the particle self-shielding bias.

4

BADGER Undetected Crack Bias ( $\Delta k_{\text{undetected cracks}}$ )

Review of the panel local dissolution effects from the Monte-Carlo analysis described in Section 4.2 indicated that each of the [ ] randomly generated panels included [ ] inches of end shrinkage. As a conservative bound, [ ]" of total gap (or [ ] – 1/3<sup>rd</sup> inch cracks) could be present as undetected cracks or local dissolution. This

4

corresponds to the maximum panel shrinkage of 4.1% or [ ] less [ ]" of end shrinkage. For this bias, it was assumed that each panel contained [ ] cracks spaced axially on [ ]" centers along the full length of the Boraflex panel. The model is infinite in the axial direction. The reactivity effect of possible undetected cracks being observed as local dissolution is [ ] as shown in Table 4-1. The reactivity effect is listed in Table 4-1 and is added directly to the reference eigenvalue as listed in Table 5-4.

4

Leakage( $\Delta k_{\text{leakage}}$ )

The reference models were infinite in all lateral and axial directions. Therefore, no credit for leakage was taken.

4

#### 5.3.4 Space Between Modules

The reference CASMO calculations assume an infinitely repeating array of storage cells in the x and y directions as shown in Figure 2-2. In the Peach Bottom spent fuel pools the individual storage cells are interconnected to form rack modules. One module typically consists of an array of 19 x 20 cells. A KENO V.a model was developed to determine reactivity effect of gaps at the module-to-module interface. Effectively, this model is an infinite array of 20 x 20 modules (modified in length for assembly drop analysis) each separated by 1.15 inch water gap in all directions. The result of this calculation indicates a net decrease in  $k_{\text{eff}}$ .

4

#### 5.3.5 Summary of Reactivity Calculations

Table 5-4 contains a summary of the criticality analyses results for the Peach Bottom Unit 2 spent fuel racks. The nominal benchmark-bias-corrected reference case  $k_{\text{eff}}$  for the GNF2 fuel at [ ] w/o containing gadolinia rods is [ ]. The results of tolerances and uncertainties when combined in a root-mean-square manner are [ ]. At a 95% probability with a 95% confidence level the maximum  $k_{\text{eff}}$  of the Peach Bottom Unit 2 fuel racks loaded with GNF2 fuel including all bias, tolerances, uncertainties and abnormal/accident conditions is [ ].

4

#### 5.3.6 Abnormal/Accident Conditions

The following abnormal/accident conditions have been evaluated in order to determine the corresponding effects on fuel pool criticality:

- Fuel Assembly Drop
- Rack Lateral Movements
- Fuel Assembly Alongside Rack
- Moderator Density and Temperature Variations

The drop of a fuel assembly with the assembly coming to rest in a horizontal or inclined position on top of the fuel and rack module has been evaluated. The resulting change in reactivity is slightly positive, however within the statistical uncertainty of the calculation ( $1\sigma$ ) it is negligible.

4

Rack lateral motion can be postulated to occur during a seismic event. The racks have been analyzed at the minimum module-to-module spacing. Since all peripheral cell walls contain Boraflex, racks in contact would have 2 panels of Boraflex between adjacent fuel bundles. Therefore, the limiting condition is the reference infinite array and there is no further increase in reactivity due to rack lateral movement during a postulated seismic event. Analysis of a 1.15-inch gap between modules resulted in a lower  $k_{eff}$  relative to the infinite array.

The inadvertent positioning or the drop of a fuel assembly along side of a rack module between the module and the pool wall has been evaluated. The maximum increase in reactivity due to a dropped bundle is [                    ] and is well within the sub-critical margin to the  $k_{eff} \leq 0.95$  limit for accident conditions as specified by Section 9.1.1 of NUREG-0800.

4

The effect of variations in moderator density and temperature on the reactivity of the Peach Bottom spent fuel storage racks have been analyzed. Loss of pool cooling has been postulated and analyzed at [     ]°F, [     ]°F and [     ]°F and results in a lower  $k_{eff}$  relative to the reference case at maximum water density. Therefore, it is concluded that under worst-case accident conditions, the effective multiplication factor remains less than the  $k_{eff} \leq 0.95$  limit, which applies to accident conditions. It should be noted that evaluation at the higher temperatures also bounds the higher moderator temperatures that occur in the spent fuel racks as a result of decay heat.

4

4

**Table 5-4**  
**Summary of Criticality Calculation Results**  
**(GNF2 Vanished 1 Lattice at 20°C\*)**

4

## 6.0 Conclusions

The Peach Bottom spent fuel racks have been analyzed for the GNF2 fuel type with uniform initial enrichments of up to [ ] w/o  $U^{235}$  at a stack density of [ ] percent theoretical density. Maximum reactivity bundles with gadolinia for this fuel type have been specified requiring a minimum number of burnable poison rods per assembly and a minimum  $Gd_2O_3$  loading per rod. Analyses have demonstrated that the maximum  $k_{eff}$  of the Peach Bottom spent fuel racks is less than 0.95 when loaded with maximum reactivity bundles of the GNF2 fuel design and accounting for projected Boraflex degradation when the peak panel boron carbide loss reaches [ ] percent.

4

4

The maximum  $k_{eff}$  of the Peach Bottom spent fuel racks will not exceed the 0.95 limit when conservatively loaded with GNF2 fuel with a maximum bundle planer enrichment of [ ] w/o  $U^{235}$  (at [ ] percent theoretical density) with a minimum of [ ] gadolinia rods per fuel assembly each containing a minimum loading of [ ] w/o  $Gd_2O_3$  and [ ] gadolinia rod containing [ ] w/o  $Gd_2O_3$ .

4

For the most reactive GNF2 lattice (Vanished1), the margin to the  $k_{eff} \leq 0.95$  design limit is [ ]. When the worst case accident is imposed upon these conditions,  $k_{eff} = [ ]$  remains below the accident condition regulatory limit of  $\leq 0.95$ . In all cases analyzed, conservative projections of Boraflex degradation were assumed.

4

In order to insure that the measured Boraflex degradation does not exceed [ ] (average) and [ ] (conservatively bounding), RACKLIFE projections should be verified with BADGER measurements.

4

Since 1996, BADGER testing has been conducted in the spent fuel pools of each unit at Peach Bottom once every four years. Comparison of BADGER measurements with RACKLIFE predictions has shown the RACKLIFE predictions to be conservative. Accordingly, it is recommended that Exelon continue this practice.

## 7.0 References

1. "An Assessment of Boraflex Performance in Spent-Nuclear-Fuel Storage Racks," Northeast Technology Corp. for the Electric Power Research Institute, NP-6159; December 1988.
2. "Boraflex Test Results and Evaluation", EPRI/TR-101986, prepared by Northeast Technology Corp. for the Electric Power Research Institute; February 1993.
3. "BADGER, a Probe for Non-destructive Testing of Residual Boron-10 Absorber Density in Spent-fuel Storage Racks: Development and Demonstration", EPRI TR-107335. Electric Power Research Institute: Palo Alto, CA; October 1997.
4. "The Boraflex Rack Life Extension Computer Code -- RACKLIFE: Theory and Numerics." EPRI TR-107333. Electric Power Research Institute: Palo Alto, CA; September 1997.
5. "The Boraflex Rack Life Extension Computer Code -- RACKLIFE: Verification and Validation." EPRI TR-109926. Electric Power Research Institute: Palo Alto, CA; March 1999.
6. "BADGER Demonstration at Peach Bottom Atomic Power Station Unit 2," NET-092-05, Rev. 0., Northeast Technology Corp. for the Electric Power Research Institute; August 1996.
7. "BADGER Test Campaign at Peach Bottom Unit 2", NET-192-01, Rev. 0., Northeast Technology Corp.: Kingston, NY; 22 May 2002.
8. " BADGER Test Campaign at Peach Bottom Unit 2", NET-264-01, Rev. 2, Northeast Technology Corp.: Kingston, NY; 21 June 2006.
9. "BADGER Test Campaign at Peach Bottom Unit 3", NET-174-01, Rev. 0, Northeast Technology Corp.: Kingston, NY; 9 July 2001.
10. "BADGER Test Campaign at Peach Bottom Unit 3", NET-247-01, Rev. 0, Northeast Technology Corp.: Kingston, NY; 6 August 2005.

11. "GNF2 Design Basis Bundle for Spent Fuel Rack Criticality Analysis at Peach Bottom Atomic Power Station Units 2 and 3," DRF Section 0000-0106-9392, Rev. 0; Class III Global Nuclear Fuel; November 2009.
12. Deleted
13. Deleted
14. "SCALE-PC: Modular Code System for Performing Criticality Safety Analyses for Licensing Evaluation, Version 5.0", Parts 1 through 3, RSIC Computer Code Collection CCC-725. Oak Ridge National Laboratory: Oak Ridge, Tennessee; May 2004.
15. Rhodes, Joel and Malte Edenius. "CASMO-4: A Fuel Assembly Burnup Program -- User's Manual", Version 2.05, Rev. 0. SSP-01/400. Studsvik of America: Newton, Massachusetts; September 2001.
16. Deleted
17. Deleted
18. Deleted
19. Deleted
20. Deleted
21. Deleted
22. Natrella, Mary Gibbions, Experimental Statistics, National Bureau of Standards Handbook 91; 1 August 1963.

4

4

23. Memorandum from L. Kopp, SRE, to Timothy Collins, Chief, Reactors System Branch, Division of Systems Safety and Analysis, "Guidance on the Regulatory Requirements for Criticality Analysis of Fuel Storage at Light Water Reactor Power Plants", August 19, 1998.
24. Deleted
25. Doub, W.B., "Particle Self-Shielding in Plates Loaded with Spherical Poison Particles," Part B of Section 4.2, Naval Reactors Physics Handbook, Volume 1: Selected Basic Techniques, Naval Reactors, Division of Reactor Development, United States Atomic Energy Commission: Washington, D.C.; 1964.

**Appendix A**

**NET-264-02 NP REV 4**  
Non-Proprietary Information Submitted in  
Accordance with 10 CFR 2.390

**Appendix A**

**NET-901-02-05, Rev 4,  
“Benchmarking of Computer Codes for  
Calculating the Reactivity State of  
Spent Fuel Storage Racks, Storage Casks and  
Transportation Casks”**

**Benchmarking of Computer Codes  
for  
Calculating the Reactivity State  
of  
Spent Fuel Storage Racks, Storage Casks and Transportation  
Casks**

NETCO, a division of Scientech, a business unit of  
Curtiss-Wright Flow Control Service Corporation  
108 North Front Street Third Floor - UPO Box 4178  
Kingston, New York 12402

Review/Approval Record

Rev.	Date	Prepared by:	Reviewed/Approved by:	Approved (QA) by:
4	12/12/17	Matthew C. Hand	Douglas P. Yocum	J. P. Maniani

Note: New Revision signature sheet initiated due to classification of Revision 4 of NET-901-02-05 as a NETCO Proprietary Document.

This document contains proprietary information of NETCO, a division of Scientech, a business unit of Curtiss-Wright Flow Control Service Corporation; it is submitted in confidence and is to be used solely for the purpose for which it was intended and returned upon request. This document is not to be reproduced, transmitted or disclosed or used otherwise without the written authorization of NETCO.

## **PREFACE**

This report documents the results of benchmark calculations of two computer codes used to compute the reactivity state of nuclear fuel assemblies in close-packed arrays. Such close-packed arrays include high density spent fuel storage racks, dry storage casks and casks for transporting nuclear fuel. The two computer codes, which were benchmarked and validated are:

- KENO V.a, which is a module of SCALE 5<sup>[1]</sup>
- CASMO-4<sup>[2]</sup>

To benchmark and validate the codes for spent fuel racks and cask evaluations, KENO was used to simulate a series of critical experiments. The calculated eigenvalues ( $k_{\text{eff}}$ ) were then compared with the critical condition ( $k_{\text{eff}} = 1.0$ ) to determine the bias inherent in the calculated values. For the KENO V.a calculation, the 238-energy group ENDF/B-V cross-section library was used. For CASMO-4, the 70-energy group cross-section library was used.

After determining the inherent biases associated with KENO V.a, both KENO V.a and CASMO-4 were used to model central assemblies within an array of select critical experiments. It is noted that CASMO-4 renders an infinitely repeating array of fuel assemblies and is generally used to generate cross-sections for core simulator models. As such, it does not lend itself directly to finite arrays of fuel rods surrounded by a reflector, as is the case in the critical experiments considered. Accordingly, the central fuel arrays of twenty-four critical experiments were modeled as infinite arrays with both KENO V.a and CASMO-4. A comparison of the KENO V.a and CASMO-4 eigenvalues provides a means to determine the CASMO-4 bias.

For the purposes of benchmarking SCALE-5.0, one-hundred and three critical experiments from the International Handbook of Evaluated Criticality Safety Benchmark

**NET- 901-02-05 NP, Rev 4**  
**Non-Proprietary Information Submitted in**  
**Accordance with 10 CFR 2.390**

Experiments<sup>[3]</sup> were selected because they closely represent typical fuel/rack geometries with neutron absorber panels. From the critical experiments above, twenty-four criticals were selected for validation of CASMO-4. The resulting models encompass the range of absorber strengths, moderator-to-fuel ratios and fuel rod geometries representative of most fuel storage rack and fuel cask configurations used today. These parameters were also selected to bound the parameters (area of applicability) of the specific system being analyzed.

**Table of Contents**

<b>Section</b>	<b>Page</b>
1.0 INTRODUCTION .....	1
2.0 BENCHMARKING - STANDARD PROBLEMS AND CONFIGURATION CONTROL .....	3
2.1 SCALE-5 Configuration Control .....	3
2.2 Sample Problems .....	3
2.3 CASMO-4 Configuration Control.....	4
3.0 STATISTICAL METHOD FOR BIAS DETERMINATION .....	5
4.0 SELECTION OF EXPERIMENTS AND AREA OF APPLICABILITY .....	7
4.1 SCALE-5 Experiments .....	8
4.2 CASMO-4 Experiments.....	9
5.0 BIAS DETERMINATION AND TREND ANALYSIS .....	15
5.1 SCALE-5 Benchmark Results.....	15
5.1.1 Identification of Trends in SCALE-5 Results .....	15
5.1.2 Determination of Bias and Bias Uncertainty.....	20
5.1.3 SCALE-5 Area of Applicability .....	22
5.2 CASMO-4 Benchmark Results .....	27
5.2.1 CASMO-4 Area of Applicability .....	30
6.0 CONCLUSIONS .....	31
7.0 REFERENCES .....	32

**NET- 901-02-05 NP, Rev 4**  
**Non-Proprietary Information Submitted in**  
**Accordance with 10 CFR 2.390**

**List of Tables**

<b>Table</b>	<b>Page</b>
Table 4-1: Critical Parameters for Selection of Benchmark Experiments .....	8
Table 4-2: Summary of SCALE-5 Critical Experiments.....	10
Table 4-3: Summary of CASMO-4 Critical Experiments.....	14
Table 5-1: Summary of SCALE-5 Critical Experiment Results .....	16
Table 5-2: SCALE-5 Trending Analysis of Linear Regression .....	20
Table 5-3: SCALE-5 Area of Applicability.....	22
Table 5-4: Critical Experiments as CASMO-4 Infinite Arrays - Results .....	29
Table 5-5: CASMO-4 Trending Analysis of Linear Regression.....	30
Table 5-6: CASMO-4 Area of Applicability .....	30

List of Figures

Figure	Page
Figure 5-1: Distribution of $k_{\text{eff}}$ versus Energy of the Average Lethargy Causing Fission .....	23
Figure 5-2: Distribution of $k_{\text{eff}}$ versus Enrichment (w/o $^{235}\text{U}$ ) .....	24
Figure 5-3: Distribution of $k_{\text{eff}}$ versus Moderator to Fuel Ratio (H/X) .....	25
Figure 5-4: Distribution of $k_{\text{eff}}$ versus Soluble Boron Concentration (ppm) .....	26

## **1.0 INTRODUCTION**

Criticality safety evaluations (i.e., calculations of the neutron multiplication factor,  $k_{\text{eff}}$ ) utilize computational algorithms to assure sub-criticality ( $k_{\text{eff}} < 1.0$ ) in complex 3-dimensional storage arrays of fissile material. In order to assure that calculated values of  $k_{\text{eff}}$  are subcritical with a given amount of confidence, an upper safety limit must be established based upon a determination of the computational method bias. The computational method (i.e., computer code) bias is determined via a statistical treatment of the difference between calculated and experimental eigenvalues for a series of critical benchmark experiments. The critical benchmark experiments used for comparison are representative of the 3-dimensional system being analyzed and to which the bias should apply.

NUREG/CR-6698 "Guide for Validation of Nuclear Criticality Safety Calculational Methodology" provides guidance for establishing a standard process for determining the computational method bias for computer codes that solve the 3-dimensional Boltzmann neutron transport equation. Establishing a standard process is important in establishing confidence in the ability of a computer code to accurately calculate  $k_{\text{eff}}$ . Also, the standard process allows any trends in  $k_{\text{eff}}$  with system parameters to be identified and any bias dependence to be appropriately handled. The basic process in determining code bias and bias uncertainty is as follows:

1. Identify computer methodology appropriate for analysis
2. Identify code analysis sequence (e.g., CSAS25, lattice cell, etc)
3. Identify appropriate critical experiments within Area of Applicability (AOA)
4. Perform benchmark calculations
5. Analyze results
  - a. Perform statistical analysis of results
  - b. Identify trends
  - c. Determine bias and bias uncertainty

**NET- 901-02-05 NP, Rev 4**  
**Non-Proprietary Information Submitted in**  
**Accordance with 10 CFR 2.390**

- d. Determine upper safety limits and tolerance bands (normal distribution) or via non-parametric method (non-normal distribution)
  - e. Identify subcritical margin
6. Identify any limitations of validation
  7. Formalize and document validation

The following sections of this report discuss the salient steps in validating the code systems used for criticality safety analysis and the determination of each code system bias. Section 2.0 describes each code system utilized and its associated configuration control. Section 3.0 describes the method for determining code bias and statistical treatment of the data. Section 4.0 describes the selection of the suite of critical experiments for the validation exercise. Section 5.0 summarizes the validation results and statistical trending analysis, as well as the Area of Applicability of the codes. Section 6.0 contains the final results and conclusions.

## **2.0 BENCHMARKING - STANDARD PROBLEMS AND CONFIGURATION CONTROL**

### **2.1 SCALE-5 Configuration Control**

The binary executable codes and associated batch files were provided by the Radiation Safety Information Computation Center (RSICC) on CD-ROM for use under the Windows operating system. In this form, the source programs can not be altered or modified. In addition to the binary executable codes, there are several supporting files which contain cross-section sets, and cross-section processing codes, etc. Prior to executing either code sequence, the user verifies the file names, creation dates, and sizes to insure that they have not been changed.

### **2.2 Sample Problems**

A suite of SCALE-5 input files with their corresponding output files were provided with each SCALE-5 code. These were executed on NETCO's host Dell Vostro workstations via batch files provided by RSICC and the resulting output files compared to those provided by RSICC on CD-ROM. Except for the date and time of execution stamps, the respective output files were identical. Each code uses a pseudo-random number generator that is initiated with a default seed value. Since the default value was used in each case, the sequences of random numbers were the same, leading to identical calculations. This verifies that the as-received versions of both codes are identical to the versions documented in the User's Manuals<sup>[1]</sup>.

Examination of the sample input decks shows that the run modules in batch files exercise all of the code options used by this benchmarking exercise. Before and after each subsequent use of each code, one set of sample input modules are executed and the output files compared to the sample output files to verify that no system degradation has occurred.

### **2.3 CASMO-4 Configuration Control**

The version of CASMO-4 used for these analyses was developed for a RISC workstation. Version 2.05.17 of CASMO-4 was used for this benchmarking work and subsequent users of CASMO-4 for NETCO will verify that Version 2.05.17 is being used. If a different version of CASMO-4 is used by NETCO for any subsequent analyses, the CASMO-4 analyses in Sections 3 thru 5 shall be repeated with the version in use.

### 3.0 STATISTICAL METHOD FOR BIAS DETERMINATION

Reference 5 defines the criteria for determining a reliable upper safety limit that are comprised from industry standard practices for validation. The basic criteria that must be satisfied is that:

$$k_{\text{calc}} + 2\sigma_{\text{calc}} < \text{USL} \quad (3-1)$$

Where:

$k_{\text{calc}}$  = calculated  $k_{\text{eff}}$

$\sigma_{\text{calc}}$  = calculated uncertainty in  $k_{\text{eff}}$

And:

$$\text{USL} = 1.0 + \text{Bias}_{\text{method}} - \sigma_{\text{method}} - \Delta_{\text{sm}} - \Delta_{\text{AOA}} \quad (3-2)$$

Where:

USL = Upper Safety Limit

$\text{Bias}_{\text{method}}$  = Methodology bias (i.e., computer code bias)

$\sigma_{\text{method}}$  = Uncertainty in the methodology bias

$\Delta_{\text{sm}}$  = Subcritical Margin (i.e.,  $0.05\Delta k$ )

$\Delta_{\text{AOA}}$  = Margin for extension beyond the Area of Applicability

Utilizing the inequality 3-1 in conjunction with equation 3-2 and simplifying (assuming no extension beyond the area of applicability), yields the familiar relation:

$$k_{\text{calc}} + 2\sigma_{\text{calc}} - \text{Bias}_{\text{method}} + \sigma_{\text{method}} < 0.95 \quad (3-3)$$

The determination of the method bias involves determining a weighted mean  $k_{\text{eff}}$  that is corrected by the factor,  $1/\sigma_t^2$ . This variance weighting reduces the importance or “weight” of experiments with larger uncertainties, both calculational and experimental, by using an effective total variance that combines both variances in the root mean square manner, as shown below:

$$\sigma_t = ( \sigma_{\text{exp}}^2 + \sigma_{\text{calc}}^2 )^{1/2} \quad (3-4)$$

The values of weighted average  $k_{\text{eff}}$ , average uncertainty of all benchmarks and weighted variance(s) are all determined using the above  $1/\sigma_t^2$  weighting factor. Ultimately, the pooled variance is determined as the square root of the sum of the squares of the weighted variance and average total uncertainty of the benchmark experiments.

The resulting methodology bias is determined by the difference between the weighted  $k_{\text{eff}}$  and the critical condition ( $k_{\text{eff}}=1$ ), or:

$$\text{Bias} = k_{\text{eff}} - 1.0 \quad (3-5)$$

In addition to determining the bias and bias uncertainty, statistical analysis of the data must be performed to determine any trends in the calculated  $k_{\text{eff}}$  or residuals. This is necessary to determine the appropriate confidence factors (used to determine the 95/95 bias and uncertainty) based on a normal distribution or non-normal (non-parametric) distribution. The statistical trend analysis is contained in Section 5.0.

#### 4.0 SELECTION OF EXPERIMENTS AND AREA OF APPLICABILITY

Typical spent fuel pools (both BWR and PWR), as well as spent fuel storage casks, contain square arrays of stainless steel fuel storage cells separated by absorber plates that contain a neutron poison (typically boron-10). Commercial nuclear fuel is typically a square lattice of cylindrical fuel rods containing uranium dioxide pellets contained within a metal cladding. In the fuel pool environment, the region outside of the fuel rod is surrounded by pure water, either borated or unborated. In order to properly validate a methodology for application to a desired system, in this case a spent fuel storage rack or cask, one must properly select benchmark experiments that most closely represent the system.

In addition to being representative of the specific system, the selected benchmarks should encompass a range of values for significant parameters that characterize that system. Table 4-1, below, contains a list of the parameters, both physical and spectral, that characterize spent fuel storage pools and casks. These parameters were used as guidance in selecting the appropriate critical experiments for this validation effort. The most significant parameters for selecting representative critical experiments for application to spent fuel pools are: (1) Fuel enrichment, (2) fuel rod lattice spacing (pitch) and (3)  $^{10}\text{B}$  loading in the absorber plates that are typical of actual rack poison loadings.

The neutron energy spectrum of the critical experiments should also be representative of the neutron spectrum that occurs in water moderated LWR fuel when surrounded by neutron absorber panels. This is effectively quantified by a parameter known as the EALF, or the average energy of the lethargy causing fission. This value was selected by comparing calculated values for typical spent fuel racks with those of the selected benchmark experiments.

**Table 4-1: Critical Parameters for Selection of Benchmark Experiments**

Characteristic or Parameter	Value Range
Material	Uranium Dioxide Cylindrical Rods
Enrichment(w/o <sup>235</sup> U)	0.71 to 5.0
Moderator	Water (pure and borated)
Lattice	Square
Pitch(cm)	1.2 to 2.0
Clad	Zircaloy (Zr-2, Zr-4, Zirlo)
Absorber material	Stainless Steel, Boron, Borated Aluminum
Moderator-to-fuel Ratio (H/U)	0 to 500
Neutron Energy Spectrum (EALF, eV)	0.1 to 3
Absorber Plate Poison Loading	w/o <sup>10</sup> B

#### 4.1 SCALE-5 Experiments

For the SCALE-5 validation, the selected critical experiments include one-hundred and three (103) water moderated LWR fuel rod cores and close packed critical LWR fuel storage arrays. Table 4-2 contains a summary description of the experimental configurations selected. Of these, 57 were conducted at the Critical Mass Laboratory at the Pacific Northwest Laboratories (PNL). Thirty-nine (39) of the PNL critical experiments were either separated by water or stainless steel (i.e., had no neutron absorber plates). The remaining 18 PNL criticals had either borated stainless steel (of varying boron weight percents) or BORAL<sup>®</sup> absorber plates separating the fuel rod arrays.

Thirty-four (34) critical experiments were performed at the Babcock & Wilcox (B&W) Lynchburg Research Center. These experiments involved 3X3 arrays of fuel rods with a uranium enrichment of 2.46 w/o. The 3X3 arrays are surrounded by borated water. Thirteen (13) different loading configurations were used depending on the separation

spacing (number of pin pitches) between fuel assemblies. Some experiments (e.g., CoreXI) merely used combinations of critical moderator height and soluble boron concentration.

The remaining 12 experiments contained mixed-oxide fuel.

The benchmark experiments were selected to be representative of typical spent fuel rack geometries and to bound the range of critical parameters listed in Table 4-1.

In each KENO model of the criticals, at least 6,000,000 neutrons in at least 3,000 generations were tracked. The output files were always checked to insure that the fission source distribution had converged.

## **4.2 CASMO-4 Experiments**

Of the 103 experiments described in Section 4.1, twenty-four (24) of these were selected for validation of CASMO-4. Twenty-two of the experiments were performed at the Babcock & Wilcox (B&W) Lynchburg Research Center. These were selected as they allowed the modeling of the central assembly of the 3 x 3 array of assemblies to be infinitely reflected. The remaining two experiments were performed at the Pacific Northwest Laboratories (PNL) and were at a higher enrichment (4.31 w/o <sup>235</sup>U). Table 4-3 contains a description of the twenty-four (24) CASMO-4 benchmark experiments.

**NET- 901-02-05 NP, Rev 4**  
**Non-Proprietary Information Submitted in**  
**Accordance with 10 CFR 2.390**

**Table 4-2: Summary of SCALE-5 Critical Experiments**

Experiment Case Name	Measured $K_{eff}$	$\sigma_{exp}$	Experiment Description	Neutron Absorber	Reflector		
<b>LEU-COMP-THERM-001</b>							
L01C01	1.000	0.0031	UO <sub>2</sub> pellets with 2.35 wt% <sup>235</sup> U. Water-reflected fuel clusters at 2.032 cm square pitch with various separation distances. No absorber plates, reflecting walls, or dissolved poison.	None	Water and acrylic plates serve as primary reflector materials. A minor contribution comes from the channel that supports the rod clusters and the 9.52 mm carbon steel tank wall.		
L01C02	1.000	0.0031					
L01C03	1.000	0.0031					
L01C04	1.000	0.0031					
L01C05	1.000	0.0031					
L01C06	1.000	0.0031					
L01C07	1.000	0.0031					
L01C08	1.000	0.0031					
<b>LEU-COMP-THERM-002</b>							
L02C01	1.000	0.0020	UO <sub>2</sub> pellets with 4.306 wt% U- <sup>235</sup> . Water-reflected fuel clusters at 2.54 cm square pitch with various separation distances. No absorber plates, reflecting walls, or dissolved poison.	None	Water and acrylic plates serve as primary reflector materials. A minor contribution comes from the channel that supports the rod clusters and the 9.52 mm carbon steel tank wall.		
L02C02	1.000	0.0020					
L02C03	1.000	0.0020					
L02C04	1.000	0.0018					
L02C05	1.000	0.0019					
<b>LEU-COMP-THERM-004</b>							
L04C01	1.000	0.0033	UO <sub>2</sub> pellets with 4.306 wt% U- <sup>235</sup> . Water-reflected fuel clusters at 1.892 cm square pitch with various separation distances. No absorber plates or reflecting walls. Dissolved gadolinium poison impurity in the water.	10.4 ± 3.6 g/m <sup>3</sup> Gd	Water and acrylic plates serve as primary reflector materials. A minor contribution comes from the channel that supports the rod clusters and the 9.52 mm carbon steel tank wall.		
L04C02	1.000	0.0033		10.4 ± 3.6 g/m <sup>3</sup> Gd			
L04C03	1.000	0.0033		10.4 ± 3.6 g/m <sup>3</sup> Gd			
L04C04	1.000	0.0033		10.4 ± 3.6 g/m <sup>3</sup> Gd			
L04C05	1.000	0.0033		10.4 ± 3.6 g/m <sup>3</sup> Gd			
L04C06	1.000	0.0033		10.4 ± 3.6 g/m <sup>3</sup> Gd			
L04C07	1.000	0.0033		10.4 ± 3.6 g/m <sup>3</sup> Gd			
L04C10	1.000	0.0035		None			
<b>LEU-COMP-THERM-009</b>							
L09C01	1.000	0.0021		UO <sub>2</sub> pellets with 4.306 wt% U- <sup>235</sup> . Water-reflected row of 3 fuel clusters (15x8) at 2.54 cm square pitch with various separation distances. Various absorber plates as indicated. No reflecting walls.		0.485 cm 304L plates	Water and acrylic plates serve as primary reflector materials. A minor contribution comes from the channel that supports the rod clusters and the 9.52 mm carbon steel tank wall.
L09C02	1.000	0.0021	0.302 cm 304L plates				
L09C03	1.000	0.0021	0.298 cm 304L plates 1.05 wt% B				
L09C04	1.000	0.0021	0.298 cm 304L plates 1.62 wt% B				
L09C05	1.000	0.0021	0.509 cm Boral plates 28.7 wt% B				
L09C06	1.000	0.0021					
L09C07	1.000	0.0021					
L09C08	1.000	0.0021					
L09C09	1.000	0.0021					

**NET- 901-02-05 NP, Rev 4**  
**Non-Proprietary Information Submitted in**  
**Accordance with 10 CFR 2.390**

**Table 4-2 (Continued): Summary of SCALE-5 Critical Experiments**

LEU-COMP-THERM-011					
L11C01	1.000	0.0018	UO <sub>2</sub> pellets with 2.459 wt% U-235. Water-reflected 3x3 array fuel clusters (14x14) at 1.636 cm square pitch with various separation distances. Various number of B4C absorber rods as indicated or soluble boron. No reflecting walls. L11C01 is a single round core	None	Water and aluminum plates serve as primary reflector materials. A minor contribution comes from the 1.27 cm aluminum tank wall. Thickness of tank bottom is not indicated.
L11C02	1.000	0.0032		1037 ppm Boron	
L11C03	1.000	0.0032		769 ppm Boron	
L11C04	1.000	0.0032		764 ppm Boron	
L11C05	1.000	0.0032		762 ppm Boron	
L11C06	1.000	0.0032		753 ppm Boron	
L11C07	1.000	0.0032		739 ppm Boron	
L11C08	1.000	0.0032		721 ppm Boron	
L11C09	1.000	0.0032		702 ppm Boron	
L11C10	1.000	0.0017		84 0.935 cm OD B <sub>4</sub> C rods 77.8 wt% B	
L11C11	1.000	0.0017			
L11C12	1.000	0.0017		64 0.935 cm OD B <sub>4</sub> C rods 77.8 wt% B	
L11C13	1.000	0.0017			
L11C14	1.000	0.0017		34 0.935 cm OD B <sub>4</sub> C rods 77.8 wt% B	
L11C15	1.000	0.0018		None	
LEU-COMP-THERM-013					
L13C01	1.000	0.0018	UO <sub>2</sub> pellets with 4.306 wt% <sup>235</sup> U. Water/steel-reflected row of 3 fuel clusters (12x16) at 1.892 cm square pitch with various separation distances. Various absorber plates as indicated. Steel reflecting walls on long sides of 3 cluster row. No dissolved poison	0.302 cm 304L plates	Water, acrylic support plates and the 17.85 cm thick steel walls serve as primary reflector materials. A minor contribution comes from the channel that supports the rod clusters and the 9.52 mm carbon steel tank wall.
L13C02	1.000	0.0018		0.298 cm 304L plates 1.1 wt% B	
L13C03	1.000	0.0018		0.216 cm Boral B plates 30.36 wt% B	
L13C04	1.000	0.0018		0.226 cm Boraflex plates 32.74 wt% B	
LEU-COMP-THERM-014					
L14C01	1.000	0.0019	UO <sub>2</sub> pellets with 4.306 wt% <sup>235</sup> U. Water/Plexiglas-reflected cluster at 1.892 cm or 1.715 cm square pitch. The Plexiglas walls are surrounded by pure water. Dissolved boron poison	None	Water, Plexiglas support plates and 1.905 cm thick Plexiglas walls serve as primary reflector materials.
L14C05	1.000	0.0069		2.55 g/L boron	
L14C06	1.000	0.0033		None	
L14C07	1.000	0.0051		1.03 g/L boron	
LEU-COMP-THERM-016					
L16C01	1.000	0.0031	UO <sub>2</sub> pellets with 2.35 wt% <sup>235</sup> U. Water-reflected row of 3 fuel clusters at 2.032 cm square pitch with various separation distances. Various absorber plates as indicated. No reflecting walls.	0.485 cm 304L plates	Water and acrylic plates serve as primary reflector materials. A minor contribution comes from the channel that supports the rod clusters and the 9.52 mm carbon steel tank wall.
L16C02	1.000	0.0031			
L16C03	1.000	0.0031			
L16C04	1.000	0.0031			
L16C05	1.000	0.0031		0.302 cm 304L plates	
L16C06	1.000	0.0031			
L16C07	1.000	0.0031			
L16C08	1.000	0.0031		0.298 cm 304L plates 1.05 wt% B	
L16C09	1.000	0.0031			
L16C10	1.000	0.0031		0.298 cm 304L plates 1.62 wt% B	
L16C11	1.000	0.0031			
L16C12	1.000	0.0031			
L16C13	1.000	0.0031		0.509 cm Boral plates 28.7 wt% B	
L16C14	1.000	0.0031			

**NET- 901-02-05 NP, Rev 4**  
**Non-Proprietary Information Submitted in**  
**Accordance with 10 CFR 2.390**

**Table 4-2 (Continued): Summary of SCALE-5 Critical Experiments**

LEU-COMP-THERM-024					
L24C01	1.000	0.0054	UO <sub>2</sub> pellets with 9.83 wt% <sup>235</sup> U. Water-reflected square core at 0.62 cm square pitch. No absorber plates, reflecting walls, or dissolved poison.	None	Water and D16 aluminum plates serve as primary reflector materials. A minor contribution comes from the 1.5 mm steel tank wall and stainless steel support rods.
LEU-COMP-THERM-042					
L42C01	1.000	0.0016	UO <sub>2</sub> pellets with 2.35 wt% <sup>235</sup> U. Water/steel-reflected row of 3 fuel clusters (20x18-25x18-20x18) at 1.684 cm square pitch and various separation distances. Various absorber plates as indicated. Steel reflecting walls on long sides of 3 cluster row. No dissolved boron	0.302 cm 304L plates	Water, acrylic support plates and the 17.85 cm thick steel walls serve as primary reflector materials. A minor contribution comes from the channel that supports the rod clusters and the 9.52 mm carbon steel tank wall.
L42C02	1.000	0.0016		0.298 cm 304L plates 1.1 wt% B	
L42C03	1.000	0.0016		0.216 cm Boral B plates 30.36 wt% B	
L42C04	1.000	0.0017		0.226 cm Boraflex plates 32.74 wt% B	
LEU-COMP-THERM-051					
L51C01	1.000	0.0020	UO <sub>2</sub> pellets with 2.459 wt% <sup>235</sup> U. Water-reflected 3x3 array fuel clusters (14x14) at 1.636 cm square pitch and various separation distances. Various absorber plates and soluble boron as indicated. No reflecting walls	143 ppm boron	Water and aluminum plates serve as primary reflector materials. A minor contribution comes from the 1.27 cm aluminum tank wall. Thickness of tank bottom is not indicated.
L51C02	1.000	0.0024		0.462 cm SS304 plates; 510 ppm boron	
L51C03	1.000	0.0024		0.462 cm SS304 plates; 514 ppm boron	
L51C04	1.000	0.0024		0.462 cm SS304 plates; 501 ppm boron	
L51C05	1.000	0.0024		0.462 cm SS304 plates; 493 ppm boron	
L51C06	1.000	0.0024		0.462 cm SS304 plates; 474 ppm boron	
L51C07	1.000	0.0024		0.462 cm SS304 plates; 462 ppm boron	
L51C08	1.000	0.0024		0.462 cm SS304 plates; 432 ppm boron	
L51C09	1.000	0.0019		0.462 cm SS304 plates; 217 ppm boron	
L51C10	1.000	0.0019		0.645 cm Al plates 1.614 wt% B; 15 ppm boron	
L51C11	1.000	0.0019		0.645 cm Al plates 1.62 wt% B; 28 ppm boron	
L51C12	1.000	0.0019		0.645 cm Al plates 1.257 wt% B; 92 ppm boron	
L51C13	1.000	0.0022		0.645 cm Al plates 0.401 wt% B; 395 ppm boron	
L51C14	1.000	0.0019		0.645 cm Al plates 0.401 wt% B; 121 ppm boron	
L51C15	1.000	0.0024		0.645 cm Al plates 0.242 wt% B; 487 ppm boron	
L51C16	1.000	0.0020		0.645 cm Al plates 0.242 wt% B; 197 ppm boron	
L51C17	1.000	0.0027		0.645 cm Al plates 0.1 wt% B; 634 ppm boron	
L51C18	1.000	0.0019		0.645 cm Al plates 0.1 wt% B; 320 ppm boron	
L51C19	1.000	0.0021		0.645 cm Al plates 0.1 wt% B; 72 ppm boron	

NET- 901-02-05 NP, Rev 4  
 Non-Proprietary Information Submitted in  
 Accordance with 10 CFR 2.390

**Table 4-2 (Continued): Summary of SCALE-5 Critical Experiments**

MIX-COMP-THERM-002					
M02C30	1.00018	0.0059	Mixture of natural UO <sub>2</sub> and 2wt% PuO <sub>2</sub> (8% <sup>240</sup> Pu). Square pitched lattices, with 1.778 cm, 2.20914 cm, or 2.51447 cm pitch in borated or pure water.	1.7 ppm Boron	Water and aluminum plates serve as primary reflector materials. A minor contribution comes from support structures.
M02C31	1.00006	0.0045		687.9 ppm Boron	
M02C32	1.00019	0.0029		0.9 ppm Boron	
M02C33	1.00022	0.0021		1090.4 ppm Boron	
M02C34	1.00096	0.0022		1.6 ppm Boron	
M02C35	1.00013	0.0024	767.2 ppm Boron		
MIX-COMP-THERM-003					
M03C1	1.000	0.0071	Mixture of natural UO <sub>2</sub> and 6.6wt% PuO <sub>2</sub> (8% <sup>240</sup> Pu). Square pitched lattices, with 1.3208 cm, 1.4224 cm, or 2.01158 cm pitch in borated or pure water.	None	Water and aluminum plates serve as primary reflector materials. A minor contribution comes from support structures.
M03C2	1.000	0.0057		None	
M03C3	1.000	0.0052		337 ppm Boron	
M03C4	1.000	0.0028		None	
M03C5	1.000	0.0024		None	
M03C6	1.000	0.0020		None	

NET- 901-02-05 NP, Rev 4  
 Non-Proprietary Information Submitted in  
 Accordance with 10 CFR 2.390

**Table 4-3: Summary of CASMO-4 Critical Experiments**

Experiment Case Name	Measured $k_{eff}$	exp	Experiment Description	Neutron Absorber	Reflector
<b>LEU-COMP-THERM-002</b>					
CASL02C4	1.000	0.0018	UO <sub>2</sub> pellets with 4.306 wt% U-235. Water-reflected fuel clusters at 2.54 cm square pitch with various separation distances. No absorber plates, reflecting walls, or dissolved poison.	None	Water and acrylic plates serve as primary reflector materials. A minor contribution comes from the channel that supports the rod clusters and the 9.52 mm carbon steel tank wall.
CASL02C5	1.000	0.0019			
<b>LEU-COMP-THERM-011</b>					
CASL11C2	1.000	0.0032	UO <sub>2</sub> pellets with 2.459 wt% U-235. Water-reflected 3x3 array fuel clusters (14x14) at 1.636 cm square pitch with various separation distances. Various number of B4C absorber rods as indicated or soluble boron. No reflecting walls.	1037 ppm Boron	Water and aluminum plates serve as primary reflector materials. A minor contribution comes from the 1.27 cm aluminum tank wall. Thickness of tank bottom is not indicated.
CASL11C3	1.000	0.0032		769 ppm Boron	
CASL11C4	1.000	0.0032		764 ppm Boron	
CASL11C5	1.000	0.0032		762 ppm Boron	
CASL11C6	1.000	0.0032		753 ppm Boron	
CASL11C7	1.000	0.0032		739 ppm Boron	
CASL11C8	1.000	0.0032		721 ppm Boron	
CASL11C9	1.000	0.0032		702 ppm Boron	
<b>LEU-COMP-THERM-051</b>					
CASL51C01	1.000	0.0020	UO <sub>2</sub> pellets with 2.459 wt% <sup>235</sup> U. Water-reflected 3x3 array fuel clusters (14x14) at 1.636 cm square pitch and various separation distances. Various absorber plates and soluble boron as indicated. No reflecting walls	143 ppm boron	Water and aluminum plates serve as primary reflector materials. A minor contribution comes from the 1.27 cm aluminum tank wall. Thickness of tank bottom is not indicated.
CASL51C02	1.000	0.0024		0.462 cm SS304 plates; 510 ppm boron	
CASL51C03	1.000	0.0024		0.462 cm SS304 plates; 514 ppm boron	
CASL51C04	1.000	0.0024		0.462 cm SS304 plates; 501 ppm boron	
CASL51C05	1.000	0.0024		0.462 cm SS304 plates; 493 ppm boron	
CASL51C06	1.000	0.0024		0.462 cm SS304 plates; 474 ppm boron	
CASL51C07	1.000	0.0024		0.462 cm SS304 plates; 462 ppm boron	
CASL51C08	1.000	0.0024		0.462 cm SS304 plates; 432 ppm boron	
CASL51C10	1.000	0.0019		0.645 cm Al plates 1.614 wt% B; 15 ppm boron	
CASL51C11	1.000	0.0019		0.645 cm Al plates 1.62 wt% B; 28 ppm boron	
CASL51C12	1.000	0.0019		0.645 cm Al plates 1.257 wt% B; 92 ppm boron	
CASL51C13	1.000	0.0022		0.645 cm Al plates 0.401 wt% B; 395 ppm boron	
CASL51C15	1.000	0.0024		0.645 cm Al plates 0.242 wt% B; 487 ppm boron	
CASL51C17	1.000	0.0027		0.645 cm Al plates 0.1 wt% B; 634 ppm boron	

## 5.0 BIAS DETERMINATION AND TREND ANALYSIS

### 5.1 SCALE-5 Benchmark Results

The critical experiments listed in Sections 4.1 were modeled with SCALE-5 and executed to determine a calculated  $k_{\text{eff}}$  and standard deviation. Table 5-1 contains a summary of the calculated  $k_{\text{eff}}$ . Also shown are four of the important parameters that characterize the spent fuel pool system, specifically EALF(eV),  $^{235}\text{U}$  enrichment (w/o), soluble boron concentration (ppm) and moderator-to-fuel ratio (H/X).

It can be seen that in only one experiment (mixed oxide experiment 002 cases 92-97) were any of the experimental  $k_{\text{eff}}$  values not at the critical condition. These cases were only slightly supercritical. Normalizing the calculated  $k_{\text{eff}}$  to account for this slight deviation from the critical condition (as suggested by NUREG/CR-6698) produces a nearly indistinguishable change to the calculated  $k_{\text{eff}}$ . This minor difference is not significant enough to cause any statistically significant trend in the data due to the experiment not being at the critical condition.

#### 5.1.1 Identification of Trends in SCALE-5 Results

Before a determination of the bias, the data must be analyzed to determine if there is any dependence of  $k_{\text{eff}}$  on any of the various critical parameters that characterize the spent fuel rack system. These parameters were listed previously in Table 4-1. Identifying any trends in the calculated  $k_{\text{eff}}$  values with the parameter values will reveal any inherent bias in the computational method. A simple way to identify any trends in the data is to use a linear regression (e.g., least squares fit) of the data using a statistical software package. Spreadsheet applications, such as Microsoft Excel, contain built in linear regression tools to perform this task.

**Table 5-1: Summary of SCALE-5 Critical Experiment Results**

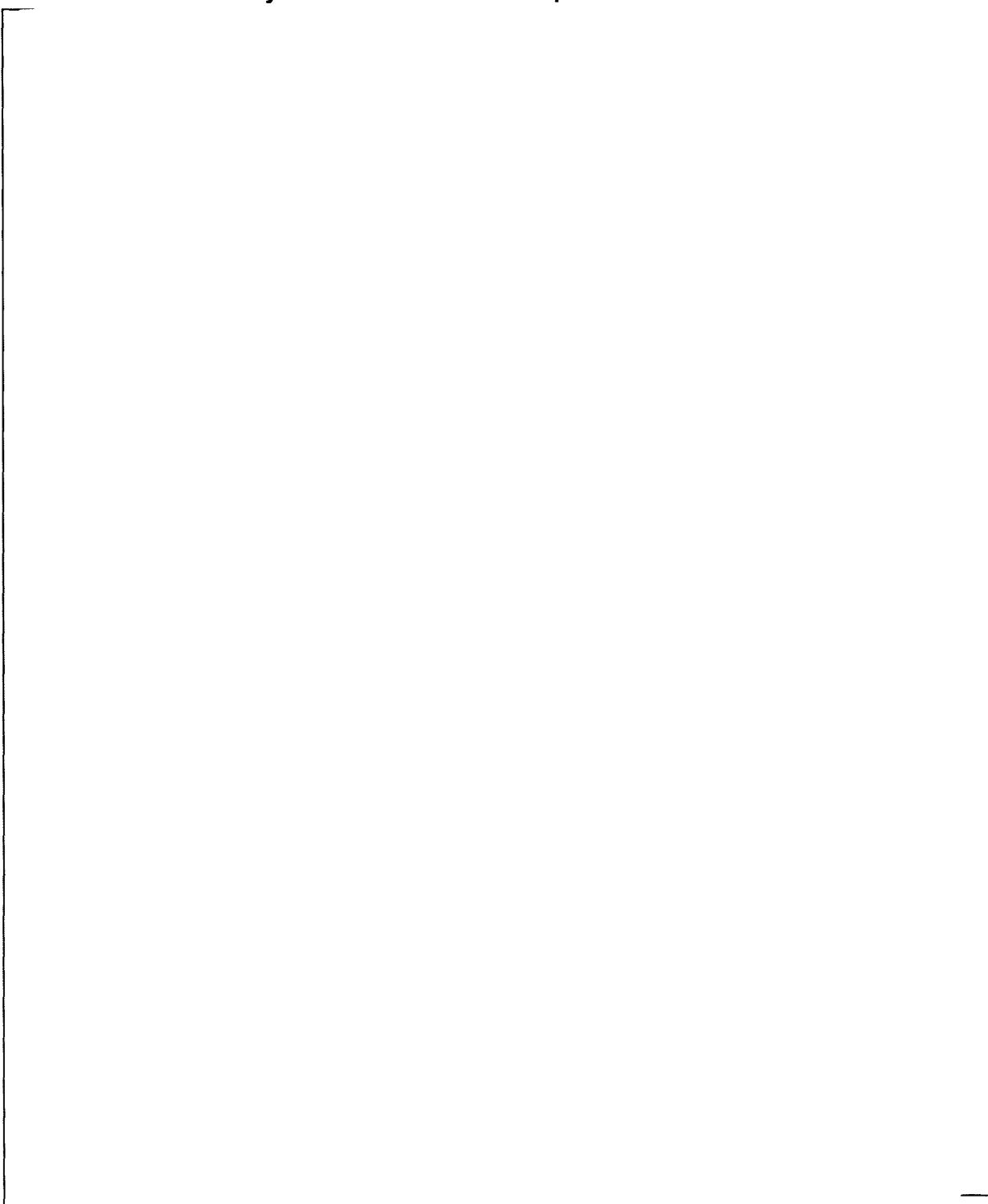


**Table 5-1 (Continued): Summary of SCALE-5 Critical Experiment Results**

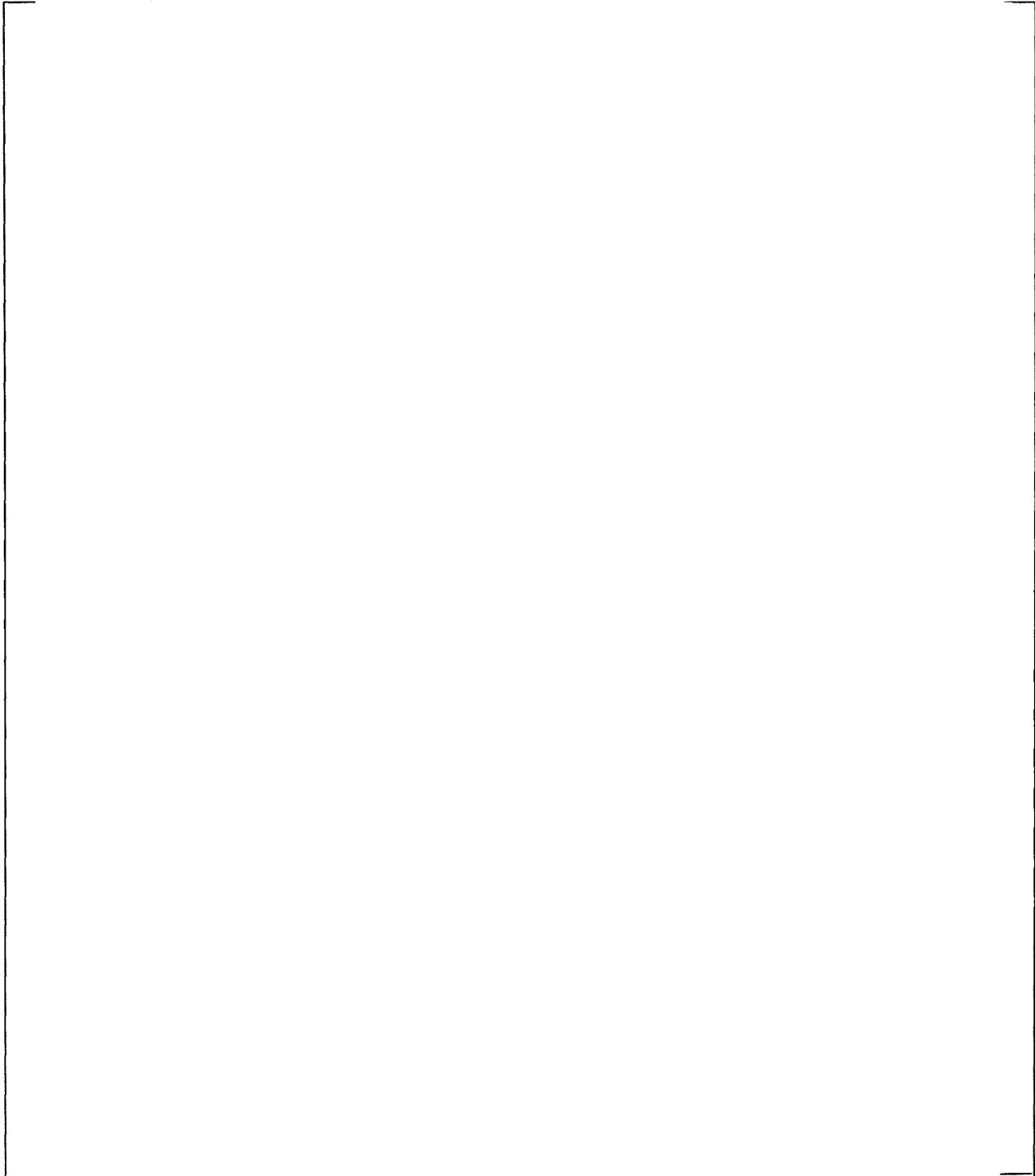


**Table 5-1 (Continued): Summary of SCALE-5 Critical Experiment Results**

A large, empty rectangular box with a thin black border, intended for the content of Table 5-1. The box is currently blank.

The least squares method of curve-fitting yields a linear equation of the form  $y(x)=mx+b$ , with slope,  $m$  and intercept,  $b$  where  $y$  is the independent variable ( $k_{\text{eff}}$ ) and  $x$  is the dependent variable (physical or spectral parameter of interest). The difference between the  $k_{\text{eff}}$  from the fit and the calculated  $k_{\text{eff}}$  is another independent variable called the 'residual'. The least squares fit of a curve also produces several statistical measures of the goodness of fit of the data, thereby giving the analyst an indicator of how well the linear equation matches experimental results. The first of these is the coefficient of determination or correlation coefficient ( $r^2$ ). It represents the fraction of the sum of the squares of the deviations in  $y(x)$  from the mean value that is due to a linear dependence of  $y$  on  $x$ . Low values of  $r^2$  ( e.g.,  $< 0.5$ ) reveal a weak linear dependence of  $x$  and  $y$ , where high values of  $r^2$  indicate a stronger linear relation between  $x$  and  $y$ .

A second measure of the viability of a linear regression model is available through the Student's T-test of the slope of a line<sup>[6]</sup>. A weak linear relation between  $x$  and  $y$  would produce a line with a slope of zero (0). A Student's T-test can be performed on the residuals assuming a null hypothesis ( $h_0: \beta_1=0$ ) that the slope is zero. The T-statistic can be calculated and compared to a critical value ( $t_{\alpha/2, n-2}$  degree of freedom). The null hypothesis (that  $\beta_1=0$ ) is rejected if  $|T| > t_{\alpha/2, n-2}$ . The results of the trend analysis (for weighted  $k_{\text{eff}}$ ) are shown in Table 5-2 below. The results of the analysis indicate that no valid trends of  $k_{\text{eff}}$  dependence on any of the parameters occur. A similar analysis of the un-weighted  $k_{\text{eff}}$  values produced similar results confirming the statistical insignificance of the trends. The P-value from the Shapiro-Wilk test also indicates low probability of the data being normal.

Figures 5-1 thru 5-4 contain plots of  $k_{\text{eff}}$  versus the trend parameters.

**Table 5-2. SCALE-5 Trending Analysis of Linear Regression**

Parameter	n	Intercept(b)	Slope (m)	r <sup>2</sup>	T	t <sub>α/2,n-2</sub>	P	Goodness of Fit Test	Valid Trend
EALF(eV)	103	0.9928	0.0023	0.003	0.95	2.27	< 1E-04	No	No
Enrichment (w/o <sup>235</sup> U)	91 <sup>+</sup>	0.9888	0.0011	0.132	3.88	2.28	< 1E-04	No	No
H/X	103	0.9890	1.7E-05	0.114	4.26	2.27	< 1E-04	No	No
Soluble boron (ppm)	103	0.9928	3.0E-6	0.034	2.62	2.27	< 1E-04	No	No

<sup>+</sup>Excludes 12 mixed oxide fuel experiments

### 5.1.2 Determination of Bias and Bias Uncertainty

NUREG/CR-6698 suggests that for data sets where no significant statistical trend can be identified, that to determine the bias of the computational methodology, it must be determined whether or not the data is normal so that proper statistical tolerances factors may be applied. The data can be subjected to one of many normality tests (e.g., Shapiro-Wilk, Anderson-Darling, etc). NUREG/CR-6698 suggests applying the Shapiro-Wilk test to generate a Q-Q plot and calculate a critical P value. The data provided in Table 5-1 were subjected to the Shapiro-Wilk test and were determined to not be normally distributed. Consequently, a non-parametric method was used to determine the bias at a 95% probability with a 95% confidence level.

Page 14 of NUREG/CR-6698 outlines a non-parametric method for determination of the 95/95 bias for non-normal distributions and any associated additional non-parametric margin that must be added to the lowest  $k_L$ . For 95% confidence, equation 32 of NUREG/CR-6698 requires a minimum of 59 critical experiments. Since the current validation effort contains 103 experiments, no additional non-parametric margin must be included.

NUREG/CR-6698 suggests determining the 95/95 bias based on the lowest ranked  $k_{eff}$  ( $k_L$ ). Reference 7 contains a table for determining the rank for  $k_L$  based on the total sample size ( $n$ ), and  $\alpha$ . For a sample size of 100, at the 95% probability and 95% confidence ( $\alpha=0.05$ ), the minimum rank to determine  $k_L$  is 2. For the data presented in Table 5-1, the  $k_{eff}$  with rank = 2 is case [ ] with a calculated  $k_{eff}$  of [ ]. The experimental uncertainty for case [ ] is  $\pm 0.0022$ . Combining the experimental uncertainty with the calculational uncertainty yields an effective total uncertainty of  $\sigma_t = \pm 0.00221$ . The resulting  $k_L$  is determined by subtracting any uncertainty from the  $k_{eff}$  with rank 2 by the following relation:

$$k_L = k_{eff,2} - \sigma_t$$

The resulting 95/95 bias is [ ] [ ]. The weighted mean  $k_{eff}$  was determined to be [ ]. The nominal bias is:

$$[ ]$$

Subtracting the nominal bias from the 95/95 bias of [ ] yields an effective 95/95 uncertainty of [ ].

### 5.1.3 SCALE-5 Area of Applicability

Table 5-3 contains a summary of the ranges of key parameters that defined the suite of critical experiments for the current validation. These parameters define the area of applicability for which the computational method is valid.

**Table 5-3: SCALE-5 Area of Applicability**

Characteristic or Parameter	Value Range
Fuel Type/Geometry	Heterogeneous arrays of Cylindrical UO <sub>2</sub> Rods
Enrichment(w/o <sup>235</sup> U)	2.35 to 9.83
Moderator	Water (pure and borated)
Lattice	Square
Pitch(cm)	0.62 to 2.54
Absorber material	Soluble Boron, Borated Plates
Moderator-to-Fuel Ratio (H/X)	41 to 398
Neutron Energy Spectrum (EALF, eV)	0.095 to 1.06

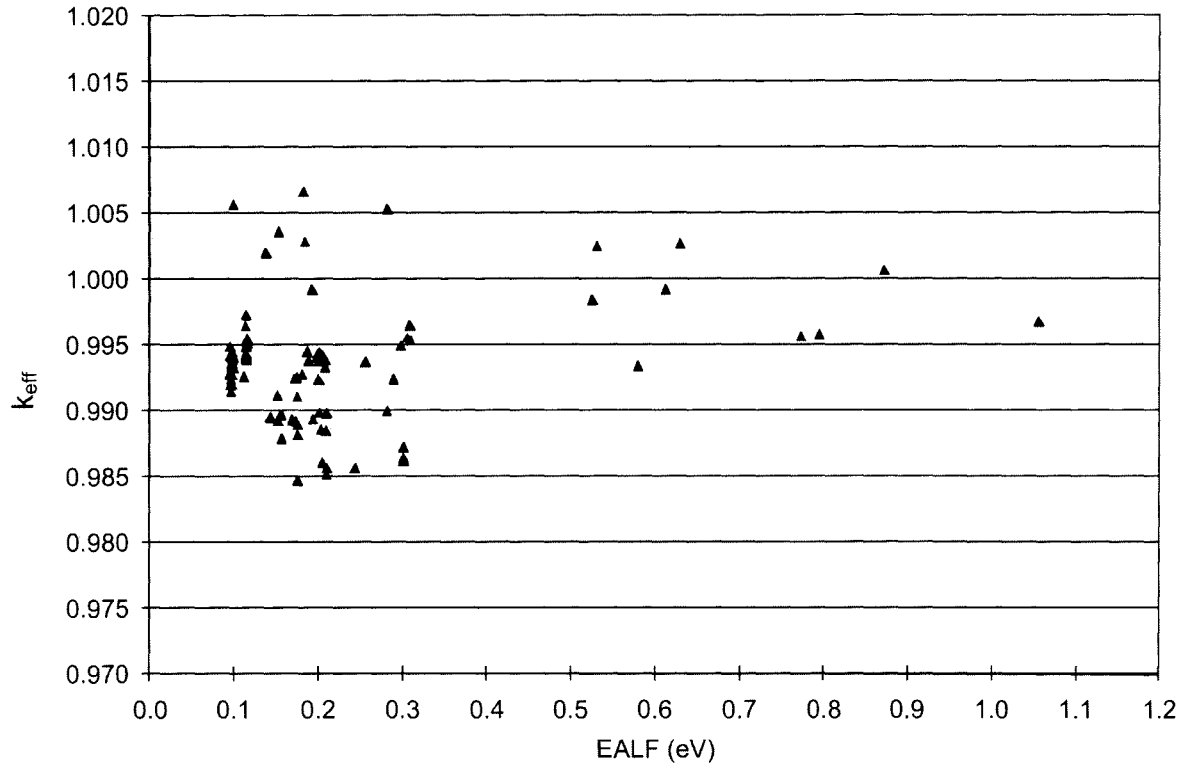


Figure 5-1. Distribution of  $k_{eff}$  versus Energy of the Average Lethargy Causing Fission



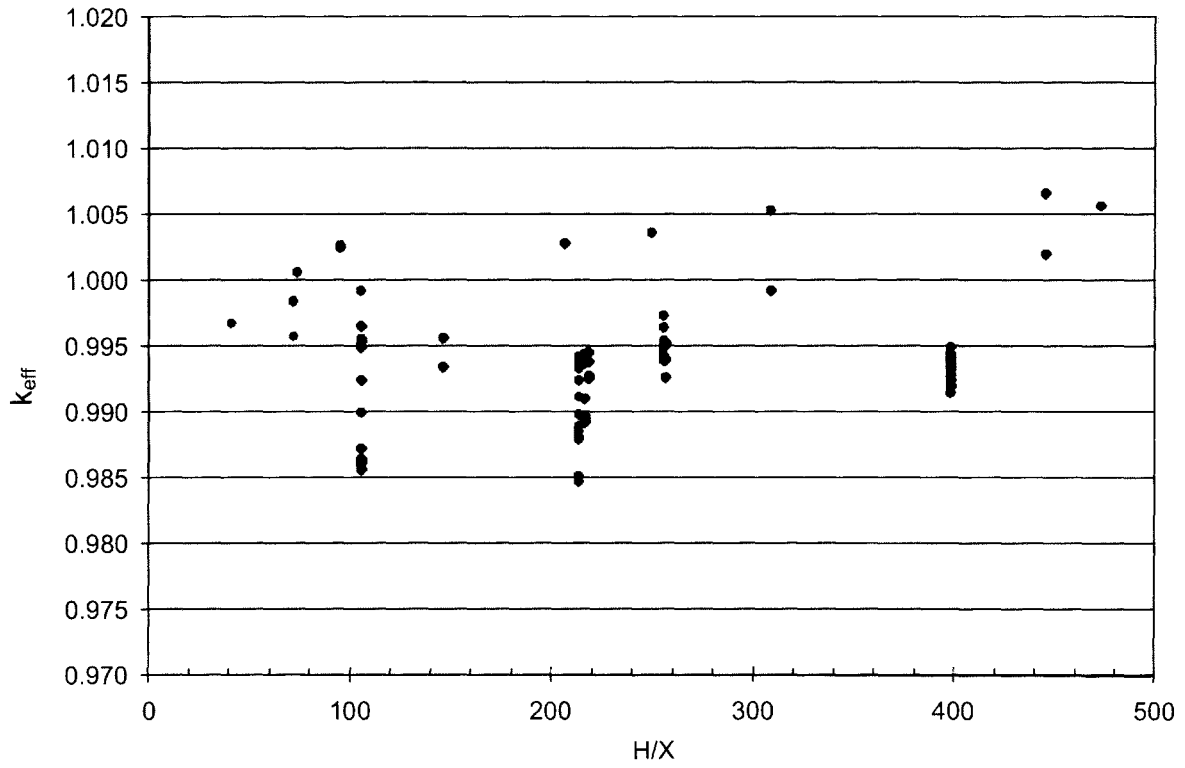
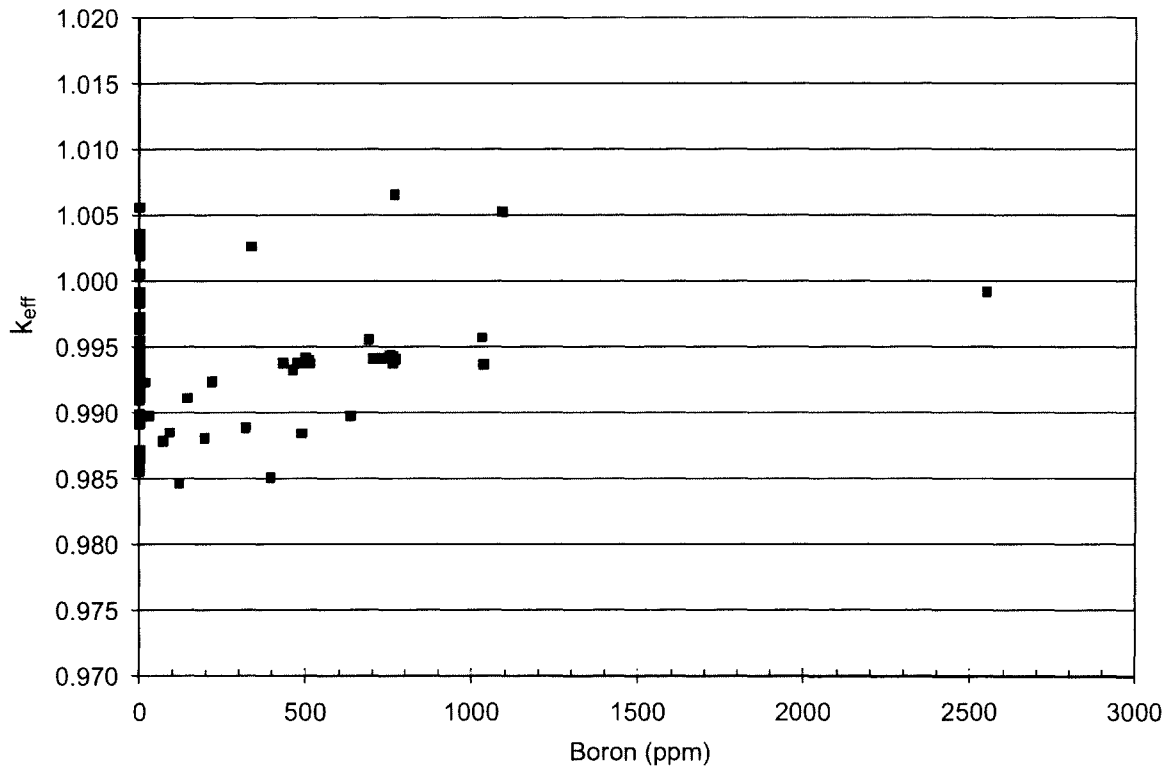


Figure 5-3. Distribution of  $k_{eff}$  versus Moderator-to-Fuel Ratio (H/X)



## 5.2 CASMO-4 Benchmark Results

This section compares SCALE-5<sup>[1]</sup> and CASMO-4<sup>[2]</sup> calculations for  $k_{\infty}$  of the twenty-two (22) B&W critical experiments<sup>[6]</sup> and two (2) PNL experiments discussed in Section 4. CASMO-4 is limited in its ability to render a 3-D geometric model and can only be used for infinite arrays of assemblies. Thus, for this benchmark analysis, the central assembly of the 3 x 3 array of assemblies in the B&W critical experiments was modeled and then assumed to be infinitely reflected. The assembly pitch was preserved in the model, but the effect of the finite water reflector around the 3 x 3 array was lost, making the model supercritical. For the two PNL criticals, the central assembly of the 3 x 1 array was modeled and infinitely reflected.

SCALE-5 was also used to model the B&W and PNL critical experiments with exactly the same geometry as they were rendered in CASMO-4. Because the bias of SCALE-5 is known (see Section 5.1.2), it can be applied to the SCALE-5 result to obtain a best-estimate of the supercritical state of the infinitely reflected assembly model. The CASMO-4 result can then be compared to obtain a CASMO-4 bias.

The results of the SCALE-5 and CASMO-4 analyses are compared in Table 5-4. The trending analysis was performed analogous to the method in Section 5.1.1 and parameters are contained in Table 5-5. The CASMO-4 bias is calculated as

$$\Delta k = k_{\text{CASMO-4}} - k_{\text{SCALE-5, bias corrected}}$$

where

$$k_{\text{SCALE-5, bias corrected}} = k_{\text{SCALE-5}} - \text{bias}_{\text{SCALE-5}}$$

The  $\Delta k$  values in Table 5-4 were tested for normality using a Shapiro-Wilk test, as well as, Anderson-Darling, Cramer-Von-Mises and Kolmogorov-Smirnoff tests. The data passed all tests and was concluded to be normally distributed.

**NET- 901-02-05 NP, Rev 4**  
**Non-Proprietary Information Submitted in**  
**Accordance with 10 CFR 2.390**

The weighted mean  $\Delta k$  between the two codes is calculated according to equation 6 of NUREG/CR-6698. The effective total uncertainty,  $\sigma_t$  is calculated as per equation 3-4. The uncertainty for SCALE-5 is the calculation uncertainty, whereas the uncertainty in CASMO-4 is taken as the convergence criteria ( $0.00001\Delta k$ ). The variance,  $s^2$ , about the weighted mean is determined per equation 4 of NUREG/CR-6698. The resulting value is  $2.542E-05$ . The average total uncertainty,  $\sigma_t$  is  $0.00017$ . Combining the two values in the root-mean-square manner yields an uncertainty about the mean [ ]. The resulting weighted mean bias is [ ].

**Table 5-4: Critical Experiments as CASMO-4 Infinite Arrays - Results**

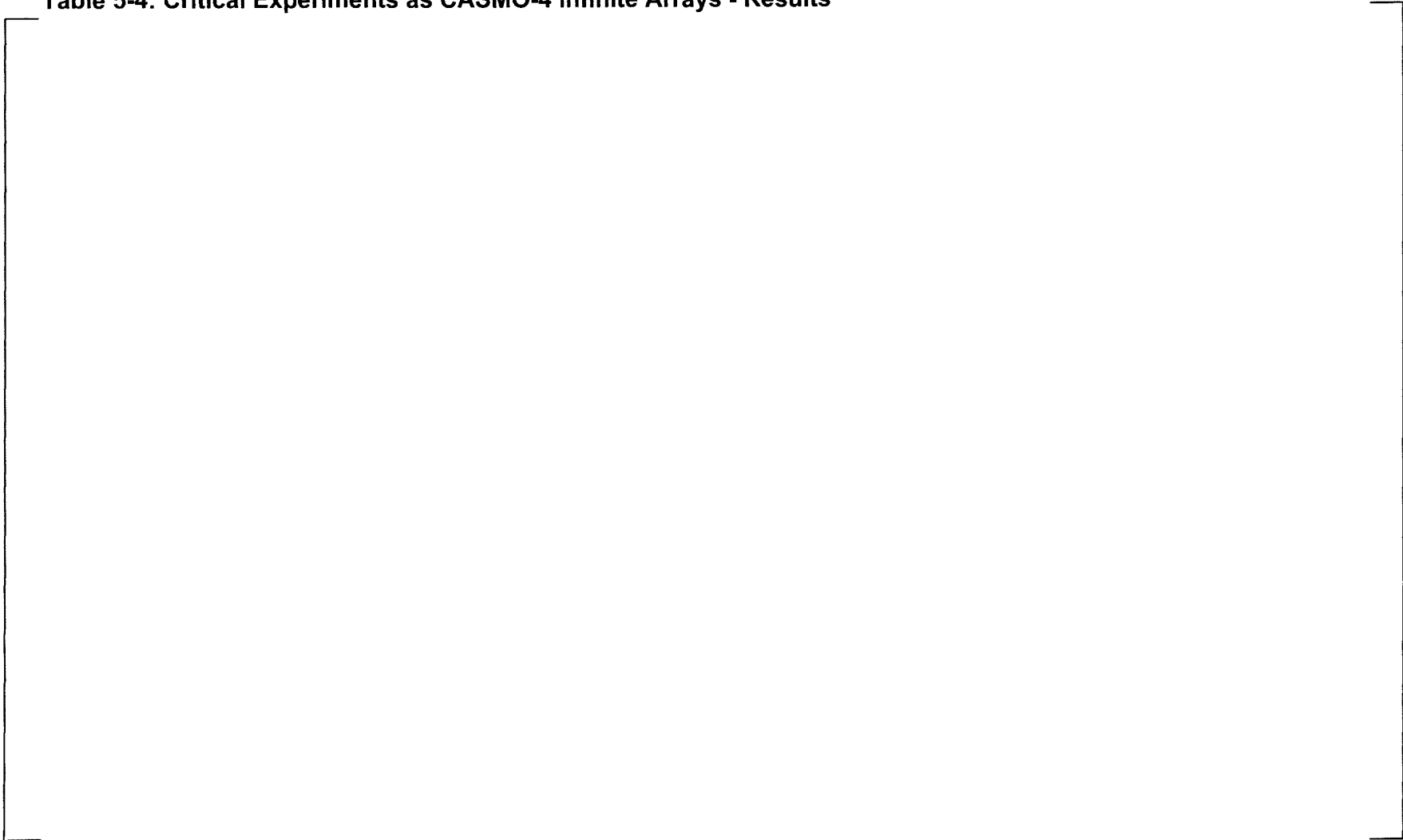


**Table 5-5. CASMO-4 Trending Analysis of Linear Regression**

Parameter	n	Intercept(b)	Slope (m)	r <sup>2</sup>	T	t <sub>α/2,n-2</sub>	P	Goodness of Fit Test	Valid Trend
EALF(eV)	24	0.0101	-0.1138	0.53	5.03	2.41	< 1E-04	No	Maybe
Enrichment (w/o <sup>235</sup> U)	24	-0.028	0.0062	0.005	-0.34	2.41	< 1E-04	No	No
H/X	24	-0.0739	0.0003	0.48	0.94	2.41	< 1E-04	No	No
Soluble boron (ppm)	24	-0.0112	0.0052	0.52	0.25	2.41	< 1E-04	No	No

### 5.2.1 CASMO-4 Area of Applicability

Table 5-6 contains a summary of the ranges of key parameters that defined the suite of critical experiments for the current validation.

**Table 5-6: CASMO-4 Area of Applicability**

Characteristic or Parameter	Value Range
Fuel Type/Geometry	Heterogeneous arrays of Cylindrical UO <sub>2</sub> Rods
Enrichment(w/o <sup>235</sup> U)	2.46 to 4.31
Moderator	Water (pure and borated)
Lattice	Square
Pitch(cm)	1.636 to 2.54
Absorber material	Soluble Boron, Borated Plates
Moderator-to-Fuel Ratio (H/U)	213.6 to 256.3
Neutron Energy Spectrum (EALF, eV)	0.11 to 0.25

## 6.0 CONCLUSIONS

SCALE-5 has been benchmarked by modeling thirty-four (34) Babcock and Wilcox critical experiments, fifty-seven (57) PNL critical experiments and twelve (12) mixed oxide (MOX) critical experiments representative of fuel storage rack and fuel cask geometries. The SCALE-5 bias with respect to these values was calculated to be [ ]. At a 95% probability / 95% confidence level, the bias uncertainty for SCALE-5 is [ ].

CASMO-4 has also been benchmarked by modeling twenty-two (22) Babcock and Wilcox and two (2) PNL critical experiments as infinite arrays. Best estimates of the  $k_{\infty}$  for the exact same geometry were calculated using SCALE-5 and applying the mean bias reported above. The CASMO-4 bias with respect to these values was calculated to be [ ] (1 sigma). At a 95% probability / 95% confidence level, the bias uncertainty for CASMO-4 is [ ] after applying a statistical one-sided confidence factor ( $n=24$ ) of 2.309. The comparison of SCALE-5 and CASMO-4 serves to verify the results of each with respect to the other.

It is therefore concluded that these calculational methods have been adequately benchmarked and validated. They may be used individually or in combination for the criticality analysis of spent fuel storage racks, fuel casks and fuel casks in close proximity to fuel storage racks, provided the appropriate biases are applied.

## **7.0 REFERENCES**

1. "SCALE-PC: Modular Code System for Performing Standardized Computer Analyses for Licensing Evaluation for Workstations and Personal Computers, Version 5," Volumes 0 through 3, RSIC Computer Code Collection CCC-725. Oak Ridge National Laboratory: Oak Ridge, Tennessee; May 2004.
2. Ekberg, Kim, Bengt H. Forssen and Dave Knott. "CASMO-4: A Fuel Assembly Burnup Program - User's Manual," Version 2.05. STUDSVIK/SSP-01/400. Studsvik of America: Newton, Massachusetts; September 2001.
3. "International Handbook of Evaluated Criticality Safety Benchmark Experiments," NEA/NSC/DOE (95)03, September 2008 Edition. Nuclear Energy Agency, September 2008.
4. "Quality Assurance Manual, Rev. 1, Northeast Technology Corp: Kingston, NY; 10 August 2007.
5. Nuclear Regulatory Commission, "Guide for Validation of Nuclear Criticality Safety Calculational Methodology", NUREG-CR/6698, January 2001.
6. Johnson, Richard A., "Inferences Based on the Least Squares Estimators," Probability and Statistics for Engineers, 6<sup>th</sup> Edition, Section 11.2. Prentice Hall: Saddle River, NJ; 2000.
7. Natrella, Mary Gibbons. Experimental Statistics, National Bureau of Standards Handbook 91. U.S. Government Printing Office: Washington, D.C.; 1 Aug. 1963.
8. "Quality Assurance Requirements of Computer Software for Nuclear Facility Applications," Part 2.7 of "Quality Assurance Requirements for Nuclear Facility Applications," ASME NQA-2-1989, Revision of ANSI/ASME NQA-2-1986. American Society of Mechanical Engineers: New York; Issued 30 September 1989.

**Appendix B**

**NET-264-02NP REV 4**  
**Non-Proprietary Information Submitted in**  
**Accordance with 10 CFR 2.390**

**Appendix B**

**Evaluation of Most Reactive Lattices in the**  
**Peach Bottom Spent Fuel Pool**

The following table contains a summary of the peak reactivity of all GE and GNF lattices that are currently in the Peach Bottom spent fuel pools. The peak lattices for the 7x7, 8x8, 9x9 and older 10x10 fuel types were provided by GNF<sup>[11]</sup>. The lattices were evaluated using CASMO-4 to determine the peak in-rack reactivity lattice (Vanished1). The table includes the peak reactivity in cold, core geometry as calculated with CASMO-4 and the GNF core design code TGBLA06. The close agreement between CASMO-4 and TGBLA06 provides confidence that CASMO-4 accurately predicts the depletion characteristics of the GE and GNF lattices. The final column in the table contains the in-rack  $k_{\infty}$  as calculated with CASMO-4. These calculations identify the GNF2 fuel type, [ ] lattice as the most reactive in rack geometry with a best estimate eigenvalue of [ ].\* This limiting lattice was the subject of the analysis described previously.

The Legacy fuel types have substantial margin relative to the design basis GNF2 fuel design. The 10x10 and 9x9 fuel arrays have similar fuel characteristics and therefore have similar neutron spectra and therefore are bounded by the design basis GNF2 lattices. The fuel enrichment/gadolinia loadings as well as the in-core  $k_{\infty}$  should be applied to future Peach Bottom fuel assemblies to assure they meet the in-rack  $k_{\infty}$ .

**Peak Reactivity GNF Lattices in the Peach Bottom Spent Fuel Racks**



**Appendix C**

**NET-264-02NP REV 4**  
**Non-Proprietary Information Submitted in**  
**Accordance with 10 CFR 2.390**

**Appendix C**  
**Area of Applicability**

**Area of Applicability**

Table C-1 contains a summary of the ranges of key parameters that bound all fuel types in the Peach Bottom spent fuel pools for the current analysis. These parameters define the area of applicability for which the computational method is valid.

**Table C-1: Peach Bottom Area of Applicability**

Characteristic or Parameter	Benchmark Value Range	Analysis Range
Fuel Type/Geometry	Heterogeneous arrays of Cylindrical UO <sub>2</sub> Rods	Same
Enrichment(w/o <sup>235</sup> U)	2.35 to 9.83	2.5 - 4.9
Moderator	Water (pure and borated)	Pure
Lattice	Square	Same
Pitch(cm)	0.62 to 2.54	1.29 - 1.87
Absorber material	Soluble Boron, Borated Plates	Borated Plates
Moderator-to-Fuel Ratio (H/U)	41 to 398	100 - 190
Neutron Energy Spectrum (EALF, eV)	0.095 to 1.06	0.1 - 0.4

**Attachment 4**

**Non-Proprietary Version of GNF-0000-0110-5796-NP, Revision 0,  
“GNF2 Design Basis Bundle for Spent Fuel Criticality Analysis at  
Peach Bottom Atomic Power Station Units 2 & 3”**



**Global Nuclear Fuel**

A Joint Venture of GE, Toshiba, & Hitachi

Global Nuclear Fuel

GNF-0000-0110-5796-NP

Revision 0

DRF Section 0000-0110-5796-R0

Class I

December 2009

*Non-Proprietary Information*

**GNF2 Design Basis Bundle for Spent Fuel Criticality Analysis**

**at**

**Peach Bottom Atomic Power Station Units 2 & 3**

*Copyright 2009 Global Nuclear Fuels-Americas, LLC  
All Rights Reserved*



## 1. Discussion

This report documents the bundle/lattice parameters required to define a GNF2 design basis bundle for performing a spent fuel storage criticality analysis in the Peach Bottom 2/3 facility. The design basis bundle/lattice is used to determine the in-rack reactivity for a given in-core reactivity. A 3-zone bundle design is provided to allow selection of the more reactive in-rack geometry relative to the in-core reactivity.

## 2. Requirements

The general requirements for a Peach Bottom 2/3 design basis bundle/lattice are shown in Table 1.

**Table 1: GNF2 Design Basis Bundle Requirements**

Parameter	Value
Bundle Design Type	GNF2
Uniform Enrichment (wt%)	4.90
Target Peak In-core Cold (20°C) Reactivity ( $k_{inf}$ )	1.270

## 3. In-core Results

Three lattice zones or types are available for use in the spent fuel storage analysis. Lattice 1 or Dominant lattice is a fully rodded zone without vanished rod locations. Lattice 2 or Vanished1 is a lattice that has six vanished rod locations. Lattice 3 or Vanished2 has fourteen vanished rod locations. Table 2 and Table 3 provide a summary of the lattice characteristics and TGBLA06 peak in-core cold reactivity results.

The in-core characteristics of the design basis bundle/lattices are generated with the GNF lattice physics system TGBLA06. To adjust the TGBLA06 evaluated in-core reactivity, a bias of [[ ]] and a 95/95 bias uncertainty of [[ ]]. This bias is based on an analysis of [[ ]] TGBLA06 to MCNP<sup>[1]</sup> comparisons over an extensive range of application for in-core depletion. The evaluated exposure range was from beginning of life (0.0 exposure) to 60.0 Gwd/st and for depletions at 0% in-channel void fractions through 70% in-channel void fractions. Typical GNF2 design configurations with lattice average enrichments from 2.96% to 4.25%, gadolinium rods from 2.0% to 7.0%, and part lengths rods

GNF-0000-0110-5796-NP Revision 0  
Non-Proprietary Information

were included in the evaluations. For fuel pool storage evaluations, the 95/95 bias uncertainty is used as a bias applied to the TGBLA in-core peak cold reactivity.

TGBLA06 and the core simulator PANAC11 were approved for use in November of 1999 and is used to provide in-core depletion characteristics for bundle assembly design, core design, reactor licensing, and core monitoring in GNF supported BWRs. It has been used to design and operate BWRs in the Finland, Germany, Japan, Mexico, Spain, Sweden, Switzerland, Taiwan, and the United States since 1999. Fuel products evaluated have ranged from 7x7 to 10x10 GNF and alternate vendor fuel products. The TGBLA06 methodology and associated licensing methodologies have been used to design and operate the Peach Bottom units since 2003. Historical evaluations of the Peach Bottom operation with TGBLA06 and PANAC11 extends back to 1992. Fuel products utilized in the Peach Bottom units since 1992 has ranged from 7x7 to 10x10 fuel designs with lattice average enrichments from 2.50% to 4.51%. The TGBLA and PANACEA methodologies have been documented in References 2, 3, 4, 5, and 6.

**Table 2: Design Basis Lattice Descriptions**

Lattice Name	Lattice No.	Lattice Type	Uniform Enrichment (%)
P10DG2L490-12G5.0-100T2-T6-555562	1	Dominant	4.90
P10DG2L490-1G6.0/11G5.0-100T2-V-T6-555563	2	Vanished1	4.90
P10DG2L490-8G5.0/4G4.0-100T2-V-T6-555564	3	Vanished2	4.90

**Table 3: Peak Cold Reactivity Results**

Lattice Number	Cold Uncontrolled In-core K-infinity	Average Exposure @ Peak $K_{inf}$ (GWD/STU)	Corrected Cold Uncontrolled In-core K-infinity (95/95)
1	[[		
2			
3			]]

#### **4. GNF2 Geometry**

Standard GNF2 design parameters are used to define the design bundle characteristics. The nominal GNF2 dimensions are provided in Table 4. The variable channel thickness variables are defined in Figures 1 and 2 below.

[[

]]

**Figure 1: GNF2 Lattice Configuration Sketch**

[[

]]

**Figure 2: GNF2 Channel Configuration Sketch**

**Table 4: Nominal Dimensions for GNF2 Fuel Lattice**

Features	Ref.	(mm)
Channel Dimensions:		
Inside Channel Width	B	[[
Corner Inside Radius	C	
Channel Corner Thickness	TCH	
[[	TCM	
	TCS	
	WML	
	WMS	
	WCS	
	WRL	
]]	WRS	
Outside Channel Gap Dimensions:		
Wide Gap	Q	
Narrow Gap	R	
Bundle Pitch*2	S	
Fuel Rod Dimensions:		
Total Cladding Thickness	D	
Outside Diameter	E	
Inside Diameter	F	
Pellet Diameter	G	
Water Rod Dimensions:		
Outside Diameter	H	
Inside Diameter	I	
Bundle Lattice Dimensions:		
Rod Pitch	M	
Rod to Rod Gap	N	
Rod to Channel Gap	O	]]

### 5. Fuel Design Tolerances

Standard GNF2 manufacturing variances recommended for use as required in the spent fuel storage criticality analysis can be found in Table 5. The manufacturing tolerance values are equivalent to a 95/95 uncertainty.

**Table 5: Tolerances for GNF2 Fuel Lattice**

Features	Value
Fuel Rod Tolerances:	
Cladding Thickness Tolerance (mm)	[[
Fuel Stack Density Tolerance (%)	
Enrichment Tolerance (wt%)	
Gadolinium Tolerance (%)	
Lattice Tolerances:	
Fuel Rod to Fuel Rod Clearance (mm)	
Pellet Tolerances:	
Fuel Pellet Diameter Tolerance (mm)	]]

## 6. Material Compositions

Isotopic compositions of water, clad, channel, SS304L, UO<sub>2</sub> material, and Gd<sub>2</sub>O<sub>3</sub> material are provided in Table 6 and Table 7. Isotopic weight fractions of Gadolinium are provided in Table 8.

**Table 6: Material Isotopic Compositions**

<b>ISOTOPICS ; 4.90w% <sup>235</sup>U</b>	
<b>Moderator at 20° C</b>	<b>Atom Density (atom/barn-cm)</b>
Oxygen	3.3370E-2
Hydrogen	6.6734E-2
<b>Cladding and Channel</b>	
Zirconium	4.32392E-2
<b>304L Stainless Steel*</b>	
Silicon	1.6728E-3
Manganese	1.4906E-2
Iron	5.6437E-2
Nickel	8.4036E-3
Manganese	1.7100E-3
<b>UO<sub>2</sub> at 4.90w% U<sup>235</sup> [(            )]</b>	
[(	
)]	
Oxygen	4.5297E-2
*Note: UO <sub>2</sub> Atom Density values assume pellet/clad contact. The nominal pellet density is reduced by the ratio of (pellet diameter/clad inner diameter) <sup>2</sup> .	

**Table 7: Gadolinium Pellet Compositions**

<b>Fuel Pellet Density</b>	
<b>Gd Concentrations (wt%)</b>	<b>Density (gm/cc)</b>
0.0	10.566
4.0	10.435
5.0	10.402
6.0	10.369

**Table 8: Gadolinium Isotopic Compositions**

<b>Gadolinium Isotopic Composition</b>							
<b>Isotope</b>	<b>Gd-154</b>	<b>Gd-155</b>	<b>Gd-156</b>	<b>Gd-157</b>	<b>Gd-158</b>	<b>Tb-159</b>	<b>Gd-160</b>
<b>Weight Fraction</b>	0.0213	0.1458	0.2030	0.1562	0.2495	0.000	0.2242

## 7. In-core Depletion Parameters

The GNF2 lattices are depleted in the infinity lattice critical configuration with the GNF standard depletion parameters. These parameters are provided in Table 9.

**Table 9: Depletion Parameters**

Depletion Conditions	
Volumetric Power Density (kw/l)	50.0
Fuel Temperature (°C)	[[      ]]
Moderator Temperature (°C)	286.0
Moderator Liquid Density (g/cc)	0.73749
Moderator Vapor Density (g/cc)	0.03733

## **8. Bundle Description**

Figure 3 contains the description of the recommended reference bundle. Three zones are provided for two-dimensional evaluation models.

[[

]]

**Figure 3: Spent Fuel Storage Analysis Design Basis Bundle**

### 9. Peak Reactivity GNF Lattices in Peach Bottom Pool

A review of the peak cold in-core reactivity of GNF bundles previously used over the life of Peach Bottom Units 2 and 3 indicates that these GNF lattices provide a bounding in-core reactivity for 7x7, 8x8, 9x9, and pre-GNF2 10x10 fuel designs. The TGBLA06 peak cold in-core reactivity for these existing lattice designs is contained in Table 10. All previous lattice designs meet a cold peak reactivity 1.270 in-core limit. The enrichment and gadolinium distributions for the lattices in Table 10 are provided in Figure 4 through Figure 10. The shaded cells identify gadolinium rod locations and the upper number in these cells identifies the  $U^{235}$  enrichment and the lower number identifies the gadolima concentration. The control blade corner or wide gap corner is in the upper left of the figures.

**Table 10: Peak Cold In-core Uncontrolled Lattice Reactivity**

GNF Lattice Name	Lattice Number	Cold K-incore
<b>7x7 Design</b>		
P7DBL250-4G3.0-80U-T6	-	[[
<b>8x8 Design</b>		
P8DWL367-5G4.0/4G3.0-80M-T6	1180	
P8DQL348-8G4.0-100M-4WR-T6	434	
<b>9x9 Design</b>		
P9HUL411-5G5.0/6G4.0-100T-V-T6	3598	
P9HUL436-12G5.0-100T-T6	3135	
<b>10x10 Design</b>		
P10DNAL451-2G7.0/10G6.0-100T-T6-8468	8468	
P10DNAL445-2G7.0/10G6.0-100T-V-T6-8470	8470	]]

[[

]]

**Figure 4: Lattice P7DBL250-4G3.0-80U-T6**

[[

]]

**Figure 5: Lattice P8DWL367-5G4.0/4G3.0-80M-T6-1180**

[[

]]

**Figure 6: P8DQL348-8G4.0-100M-4WR-T6-434**

[[

]]

**Figure 7: Lattice P9HUL411-5G5.0/6G4.0-100T-V-T6-3598**

[[

]]

**Figure 8: Lattice P9HUL436-12G5.0-100T-T6-3135**

[[

]]

**Figure 9: Lattice P10DNAL451-2G7.0/10G6.0-100T-T6-8468**

[[

]]

**Figure 10: Lattice P10DNAL445-2G7.0/10G6.0-100T-V-T6-8470**

## 10. References

1. LA-UR-03-1987, "MCNP — A General Monte Carlo N-Particle Transport Code, Version 5", April 24, 2003 (Revised 10/3/05)
2. Letter from S.A. Richards (NRC) to G.A. Watford (GE) Subject: "Amendment 26 to GE Licensing Topical Report NEDE-24011-P-A, GESTAR II Implementing Improved GE Steady-State Methods," (TAC NO. MA6481), November 10, 1999
3. NEDE-24011-P-A-16, "General Electric Standard Application for Reactor Fuel (GESTAR II)", October 2007.
4. NEDE-30130-P-A, "Steady State Nuclear Methods", April 1, 1985.
5. NEDC-33173P, "Applicability of GE Methods to Expanded Operating Domains", February 2006.
6. NEDC-33239P Rev. 2, "GE14 for ESBWR Nuclear Design Report", April 2007

**Attachment 5**

**Revised No Significant Hazards Consideration**

### **4.3 No Significant Hazards Consideration**

Exelon has evaluated whether or not a significant hazards consideration is involved with the proposed amendment by focusing on the three standards set forth in 10 CFR 50.92, "Issuance of amendment," as discussed below:

**1. Does the proposed amendment involve a significant increase in the probability or consequences of an accident previously evaluated?**

Response: No

The proposed change is to revise the k-infinity value contained in TS 4.3.1.1.a. The k-infinity value will be revised to 1.270. This change is necessary as a result of the ongoing degradation of the Boraflex neutron absorbing material. As demonstrated through the criticality analysis, the PBAPS spent fuel storage racks satisfy the reactivity requirements for all storage conditions with GNF2 fuel having an associated in-core peak k-infinity of no greater than 1.270. This change does not involve any plant modifications or operational changes that could affect system reliability, performance, or the possibility of an operator error. The fuel storage k-effective subcriticality design limit of 0.95 will continue to be required by TS 4.3.1.1.b. Therefore, the k-infinity parameter may be revised without impacting the probability or consequences of a previously evaluated accident. Additionally, a program has been established to monitor Boraflex degradation. The PBAPS, Units 2 and 3 Boraflex monitoring program discussed in our response to Generic Letter 96-04 for PBAPS, Units 2 and 3 will ensure that the spent fuel pool racks remain capable of performing their intended safety function. This change does not affect any postulated accident precursors and does not affect the performance of any accident mitigation systems that could increase the probability or consequences of an accident. Additionally, this change does not introduce any new accident initiation mechanisms.

Therefore, the proposed change does not involve an increase in the probability or consequences of an accident previously evaluated.

**2. Does the proposed amendment create the possibility of a new or different kind of accident from any accident previously evaluated?**

Response: No

The proposed change is to revise the k-infinity value contained in TS 4.3.1.1.a. The design basis for preventing fuel criticality in fuel storage facilities is not impacted by this change. This design function of the spent fuel racks will be maintained. The criticality analysis criteria being retained in TS 4.3.1.1 and 4.3.1.2, will preserve existing criticality margins associated with the storage of new and irradiated fuel. The fuel storage k-effective subcriticality design limit of 0.95 will continue to be required by TS 4.3.1.1.b. This change does not involve any plant modifications or operational changes that could affect system reliability or performance. No new failure mechanisms, malfunctions, or accident initiators will be introduced as a result of this change.

Therefore, the proposed change does not create the possibility of a new or different kind of accident from any accident previously evaluated.

**3. Does the proposed amendment involve a significant reduction in a margin of safety?**

Response: No

The proposed change is to revise the k-infinity value contained in TS 4.3.1.1.a. The k-infinity value will be revised to 1.270. This change is necessary as a result of the ongoing degradation of the Boraflex neutron absorbing material. Since the existing in-rack k-effective criteria remains consistent with fuel storage criticality design criteria, the k-infinity parameter may be revised without impacting nuclear safety. As demonstrated through the criticality analysis, the PBAPS spent fuel storage racks satisfy the reactivity requirements for all storage conditions with GNF2 fuel having an associated in-core peak k-infinity of no greater than 1.270. The criticality analysis criteria being retained in Technical Specifications 4.3.1.1 and 4.3.1.2 will preserve required criticality margins associated with the storage of new and irradiated fuel.

Therefore, the proposed change does not involve a significant reduction in a margin of safety.

Based upon the above, Exelon Generation Company, LLC concludes that the proposed amendment presents no significant hazards consideration under the standards set forth in 10 CFR 50.92(c), and, accordingly, a finding of no significant hazards consideration is justified.

**4.4 Conclusions**

In conclusion, based on the considerations discussed above, (1) there is reasonable assurance that the health and safety of the public will not be endangered by operation in the proposed manner, (2) such activities will be conducted in compliance with the Commission's regulations, and (3) the issuance of the amendment will not be inimical to the common defense and security or to the health and safety of the public.

**Attachment 6**

**Markup of Proposed Technical Specification Page Changes**

**Peach Bottom Atomic Power Station, Units 2 and 3  
Revised TS Pages  
Units 2 and 3  
4.0-2**

## 4.0 DESIGN FEATURES (continued)

---

### 4.3 Fuel Storage

#### 4.3.1 Criticality

4.3.1.1 The spent fuel storage racks are designed and shall be maintained with:

- a. Fuel assemblies having a maximum k-infinity of ~~1.362~~ in the normal reactor core configuration at cold conditions;
- b.  $k_{eff} \leq 0.95$  if fully flooded with unborated water, which includes an allowance for uncertainties as described in Section 10.3 of the UFSAR; and
- c. A nominal 6.280 inch center to center distance between fuel assemblies placed in the storage racks.

1.270

4.3.1.2 The new fuel storage racks shall not be used for fuel storage. The new fuel shall be stored in the spent fuel storage racks.

#### 4.3.2 Drainage

The spent fuel storage pool is designed and shall be maintained to prevent inadvertent draining of the pool below plant elevation 219 ft.

#### 4.3.3 Capacity

The spent fuel storage pool is designed and shall be maintained with a storage capacity limited to no more than 3819 fuel assemblies.

---

#### 4.0 DESIGN FEATURES (continued)

---

### 4.3 Fuel Storage

#### 4.3.1 Criticality

4.3.1.1 The spent fuel storage racks are designed and shall be maintained with:

- a. Fuel assemblies having a maximum k-infinity of ~~1.362~~ in the normal reactor core configuration at cold conditions;
- b.  $k_{eff} \leq 0.95$  if fully flooded with unborated water, which includes an allowance for uncertainties as described in Section 10.3 of the UFSAR; and
- c. A nominal 6.280 inch center to center distance between fuel assemblies placed in the storage racks.

1.270

4.3.1.2 The new fuel storage racks shall not be used for fuel storage. The new fuel shall be stored in the spent fuel storage racks.

#### 4.3.2 Drainage

The spent fuel storage pool is designed and shall be maintained to prevent inadvertent draining of the pool below plant elevation 219 ft.

#### 4.3.3 Capacity

The spent fuel storage pool is designed and shall be maintained with a storage capacity limited to no more than 3819 fuel assemblies.

---